

# ADVANCING VEGETATION MONITORING WITH VIRTUAL LASER SCANNING OF DYNAMIC SCENES (VLS-4D): OPPORTUNITIES, IMPLEMENTATIONS AND FUTURE PERSPECTIVES

A NON-PEER REVIEWED EARTHARXIV PREPRINT

**Hannah Weiser**

3DGeo Research Group, Institute of Geography  
Interdisciplinary Center for Scientific Computing (IWR)  
Heidelberg University  
Heidelberg, Germany

**Bernhard Höfle**

3DGeo Research Group, Institute of Geography  
Interdisciplinary Center for Scientific Computing (IWR)  
Heidelberg University  
Heidelberg, Germany

## ABSTRACT

1 1. Virtual Laser Scanning (VLS) is an established and valuable research tool in forestry and ecology, widely  
2 used to simulate labelled LiDAR point cloud data for sensitivity analysis, model training and method testing.  
3 In VLS, vegetation has traditionally been modelled as static, neglecting the influence of vegetation dynamics  
4 on LiDAR point cloud representations and limiting applications to mono-temporal analyses.

5 2. In this review, we formalise VLS-4D, a framework that extends traditional VLS by using dynamic  
6 (i.e., 4D: 3D + time) input scenes. This advancement has opened new avenues for research on vegetation  
7 monitoring. We outline key concepts for representing dynamic scenes in LiDAR simulations, review technical  
8 implementations, and present innovative VLS-4D applications.

9 3. We find that current simulation frameworks suitable for vegetation applications do not yet fully support  
10 dynamic scenes. While LiDAR time series of vegetation growth can be generated from static scene snapshots,  
11 simulating the effects of vegetation movement during a scan remains a challenge. We group the reviewed  
12 applications of VLS-4D into three key methodological areas: i) investigating LiDAR data acquisition and  
13 vegetation movement effects, ii) testing and validating new methods for change detection and analysis, and iii)  
14 generating labelled training data for machine and deep learning.

15 4. We recommend that future efforts focus on extending the functionality of current LiDAR simulators and  
16 increasing the availability of open-source tools for modelling dynamic vegetation to enable more realistic  
17 simulations. Used as a complement, not a replacement, to real data, VLS-4D has the potential to significantly  
18 advance LiDAR-based vegetation monitoring by improving our understanding of point cloud representations,  
19 enabling reliable algorithm validation, and providing high-quality training data for deep learning.  
20

21 **Keywords** 3D Animation · LiDAR Simulation · Machine Learning · Point Cloud Change Analysis · Synthetic Training Data ·  
22 Vegetation Dynamics · Vegetation Monitoring · Virtual Laser Scanning

## 23 1 INTRODUCTION

24 Understanding vegetation and its dynamics is crucial in our rapidly changing world, as vegetation underpins a wide range of  
 25 ecosystem services essential for human well-being. Among remote sensing technologies for vegetation monitoring, Light De-  
 26 tection and Ranging (LiDAR) stands out for its ability to capture the full 3D structure of vegetation because the laser beam can  
 27 penetrate canopies. Researchers use repeated LiDAR acquisitions from ground-based and airborne platforms to assess tree health  
 28 and damage [Coops *et al.*, 2009; Jacobs *et al.*, 2022; Wulder *et al.*, 2009], vegetation growth [Bienert *et al.*, 2024; Tompalski  
 29 *et al.*, 2021; Zhao *et al.*, 2018], and plant physiology [Herrero-Huerta *et al.*, 2018; Ziinszky *et al.*, 2017].

30 Each LiDAR acquisition produces a unique 3D point cloud representation, from which vegetation properties such as shape, struc-  
 31 ture, and vitality can be derived. However, point cloud representations of the exact same scene can vary significantly depending  
 32 on the acquisition parameters, affecting point distribution, density, occlusions, ranging accuracy and noise levels [Soudarissanane  
 33 *et al.*, 2011]. Directly relating point clouds to biological and physical characteristics of plants is therefore challenging, especially  
 34 without reliable reference data. Fig. 1 illustrates how a decrease in flight altitude alone can make vegetation appear much denser.  
 35 In change analysis, multi-temporal LiDAR data captured with different sensors or settings complicates distinguishing between  
 36 LiDAR acquisition effects (Fig. 1a and b) and actual change signals (Fig. 1c and d).

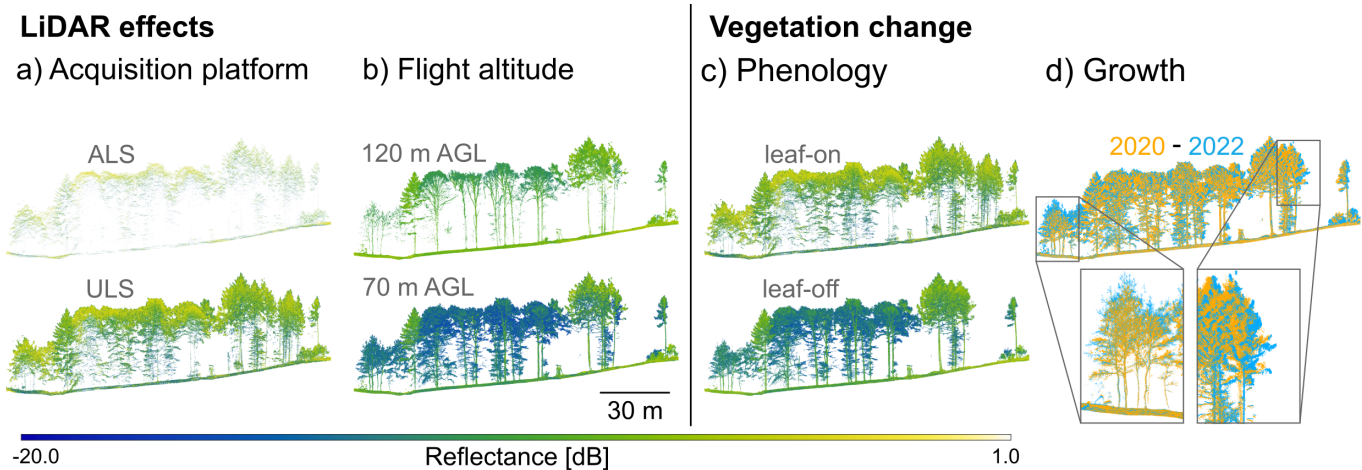


Figure 1: Real-world point cloud cross-sections demonstrating how LiDAR acquisition parameters (left) and vegetation changes (right) affect LiDAR representations. a) Acquisition platform and sensor: ALS vs. ULS, acquired approximately two months apart; b) Flight altitude: ULS on the same day and with the same device, but different flight altitudes and trajectories; c) Phenology: ULS with the same sensor and survey settings, but in leaf-on conditions and leaf-off conditions; d) Vegetation growth: Bi-temporal ULS point clouds acquired two years apart. ALS = airborne laser scanning, ULS = UAV-borne laser scanning, AGL = above ground level.

37 Uncertainty in the measurements arises not only from acquisition settings but also from vegetation movement during acquisition,  
 38 compromising data quality. In mono-temporal Terrestrial Laser Scanning (TLS), for example, branch movement manifests as  
 39 distortions in individual scans (Fig. 2a) or as duplication of branches ('ghosting effects'; Wilkes *et al.*, 2017 or 're-occurrence';  
 40 Medic *et al.*, 2023) in merged scans (Fig. 2b). These effects can result in unnoticed errors in downstream tasks (co-registration,  
 41 vegetation parameter estimation, etc.). While Medic *et al.* [2023] propose several solutions to this problem, they emphasise that  
 42 further scientific effort is required to adopt and develop these approaches.

## Movement within acquisitions

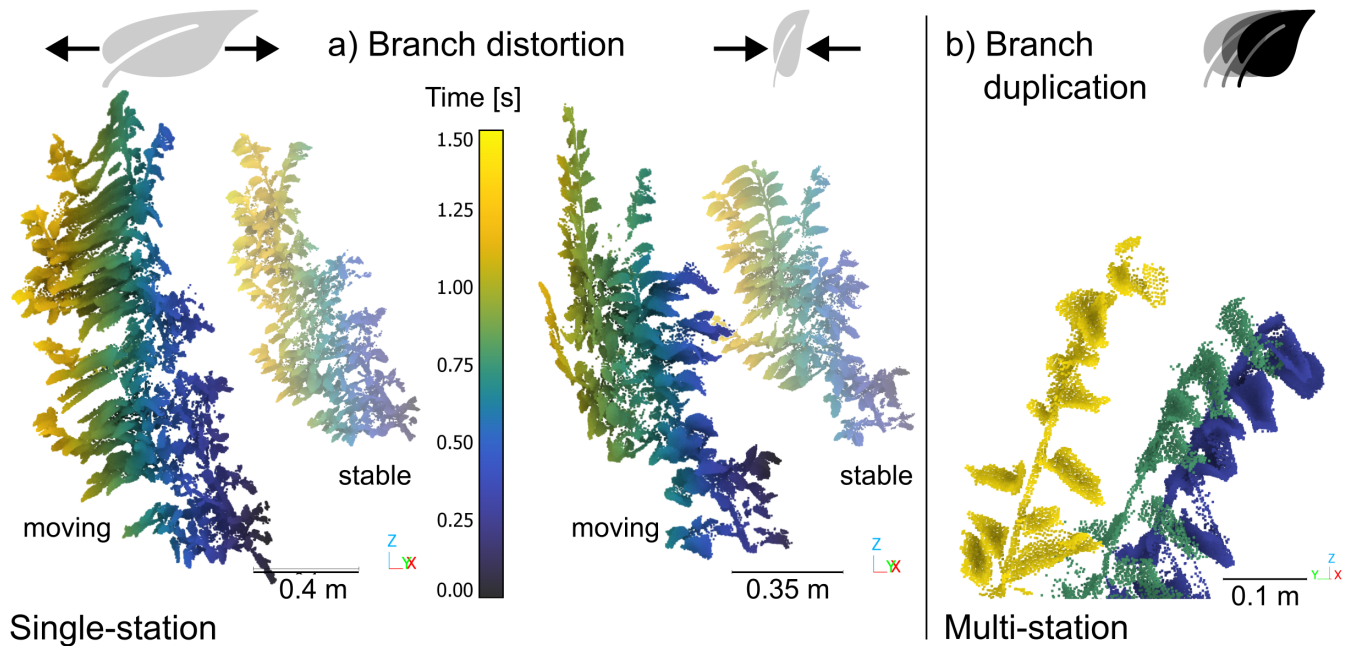


Figure 2: Examples of wind effects in terrestrial laser scanning point clouds due to branch movement during acquisition. a) Branch distortion, showing stretching (left) and compression (right) in a single scan from one station. The smaller semi-transparent images on the right show the same branches scanned under stable conditions for comparison. b) Branch duplication in a merged point cloud from multiple scan stations, with distinct colours indicating individual scans.

43 In machine learning (ML) applications, the effects of sensor, survey settings and wind on analysis results can be mitigated  
 44 by training models on large datasets that incorporate these influences (e.g., [Puliti et al., 2025](#) for species recognition). This  
 45 approach involves substantial efforts for data acquisition, processing, and labelling and remains largely unexplored in the context  
 46 of vegetation change analysis. In addition, these costly benchmark datasets can quickly become outdated and less valuable as new  
 47 LiDAR sensor systems are developed rapidly. To better understand the relationships between survey parameters, plant dynamics  
 48 and point cloud representations, controlled experiments and sensitivity analyses offer valuable insights [[Hopkinson, 2007](#)]. In  
 49 practice, the resources for empirical experiments are often too limited to comprehensively explore the input space of acquisition  
 50 parameters and environmental settings. Also, since fully replicating a given LiDAR acquisition is impossible, unavoidable  
 51 variations in survey characteristics make it difficult to isolate the effects of individual variables [[Roberts et al., 2020](#)].

52 Due to these limitations, researchers have added LiDAR simulation as an additional research tool to their studies to investigate the  
 53 influence of scanning configurations [[Hämmerle et al., 2017](#); [Roberts et al., 2020](#); [Stocker et al., 2023](#)], to validate methods for  
 54 quantifying forest biometrics [[Jiang et al., 2021](#); [Wu et al., 2021](#); [Zhu et al., 2020](#)], or to generate training data for segmentation  
 55 tasks [[Bryson et al., 2024](#); [Esmoris et al., 2024](#); [Liu et al., 2025](#)]. LiDAR simulation, or Virtual Laser Scanning (VLS), comes  
 56 with error-free reference data on scene geometry and semantics, enables the controlled variation of individual parameters, and  
 57 lets us create scenarios that mimic real or fictional acquisitions [[Winiwarter et al., 2022b](#)]. In addition, VLS does not face many  
 58 of the challenges associated with real data acquisition, such as high costs, labelling difficulties, inaccessibility of study sites, or  
 59 the limitation to specific available or affordable hardware [[Liu et al., 2025](#)]. VLS is a scientific tool that perfectly complements  
 60 and interacts with real data in a feedback loop. Real data guides the development of dynamic digital LiDAR twins and to assess

61 their realism. In turn, simulated data helps to improve experimental designs, operational field campaigns, and computational  
 62 methods for real-world data.

### Performing a LiDAR survey using simulation

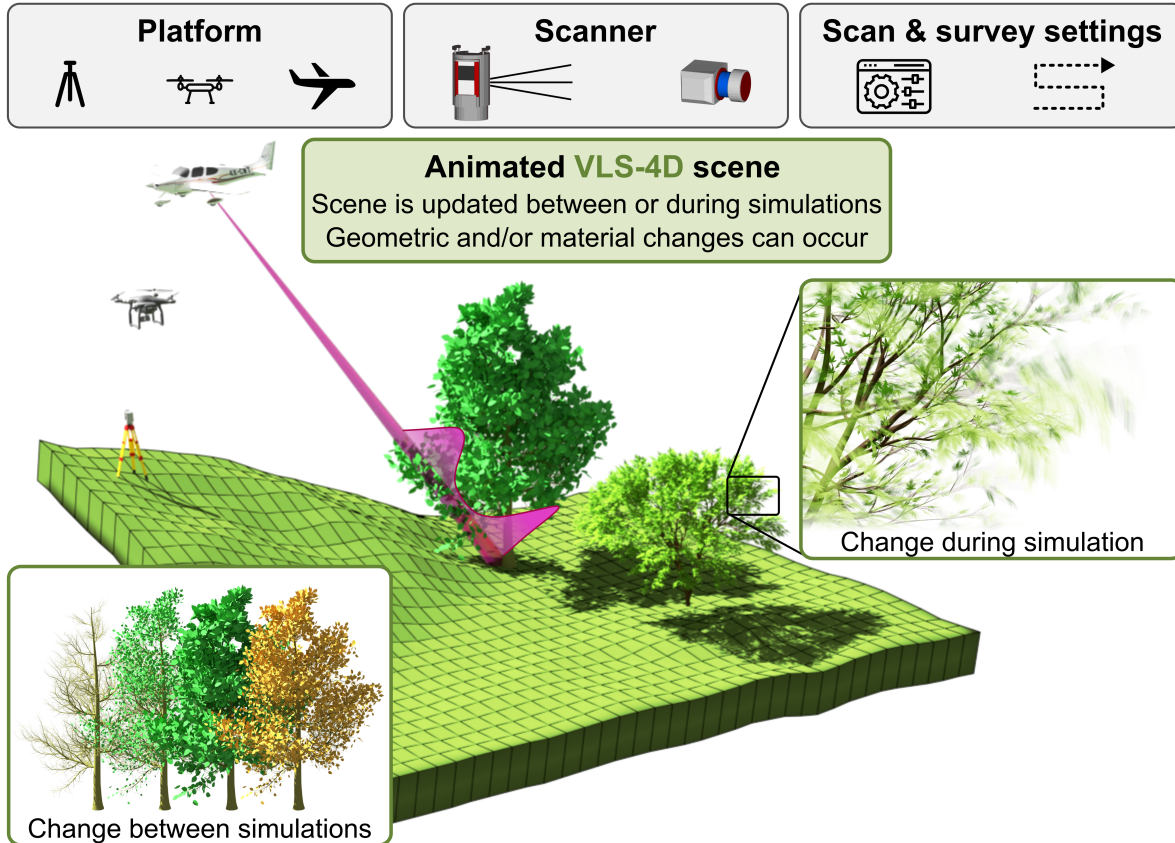


Figure 3: Schematic overview of the core modules (boxes) of VLS: The platform, the scanner which is mounted on the platform, the scan and survey settings and the scene. The novelty about VLS-4D is that the scene is dynamic (green outlined boxes). The rendered scene in the background is a modified version of Fig. 1 published in *Winiwarter et al. [2022b]* under the CC BY 4.0 licence (<https://creativecommons.org/licenses/by/4.0/>).

63 Over the past decade, VLS has become invaluable in forestry and ecology [*Bornand et al., 2024; Cai et al., 2024; Disney et al.,*  
 64 *2010; Hämmerle et al., 2017; Liu et al., 2019, 2025; Li et al., 2021b; Liu et al., 2022; Roberts et al., 2020; Schäfer et al., 2023;*  
 65 *Wang, 2020; Wang et al., 2022; Wu et al., 2021; Zhao et al., 2023*]. In most previous studies, VLS has been operated in a  
 66 ‘frozen’ world where vegetation is assumed to be completely static. This simplification limits VLS to mono-temporal scenarios  
 67 and neglects effects from the interactions between laser scanning and dynamic vegetation (Fig. 2). Moving to dynamic scenes,  
 68 VLS can help us learn how different types of plant dynamics become visible in both mono-temporal and 4D point clouds (i.e.,  
 69 point cloud sequences;  $4D = 3D + \text{time}$ ) in different scenarios. This is highly relevant to virtually anyone using laser scanning in  
 70 vegetated areas, as vegetation dynamics inherently affect real laser scanning data. These effects can either be the primary focus of  
 71 analysis or introduce unwanted variability that impacts data quality. We therefore propose advancing traditional VLS (VLS-3D)  
 72 to the concept of VLS-4D, in which objects change between or during virtual laser scans (Fig. 3). This new framework will push  
 73 progress in 4D analysis of vegetation point clouds and has the potential to make laser scanning simulations more realistic.

VLS-4D realism is majorly influenced by two factors: a) the level of detail of the scene (geometry and dynamics) and b) the fidelity of the LiDAR simulation. For a), previous LiDAR simulation studies have modelled trees using simple crown archetypes [Calders *et al.*, 2013] or geometrically detailed 3D models [Calders *et al.*, 2018]. Likewise, plant dynamics can be implemented in a very simple way, e.g. by scaling whole plants, or in a very detailed way, e.g. by including the precise movement and deformation of individual branches. For b), the fidelity of the LiDAR simulation depends largely on the representation of realistic scan patterns and the modelling of beam divergence, which determines whether multiple returns can be recorded in the canopy [Disney *et al.*, 2010; Manivasagam *et al.*, 2023]. The appropriate degree of simplification of each component ultimately depends on the specific research objectives.

As VLS-4D has not yet been formulated as a scientific method and its application in vegetation studies is still in its early stages, the objectives of this review are as follows:

- to develop a conceptual framework for VLS-4D with respect to different types of vegetation dynamics and measurement scenarios (Section 2)
- to give an overview of tools for implementing VLS-4D, from modelling dynamic plants and ecosystems to conducting LiDAR surveys in a virtual environment (Section 3)
- to identify the main methodological areas for VLS-4D and review research questions in ecology and forestry where VLS-4D can have an impact (Section 4)
- to discuss remaining challenges and identify future developments that could make VLS-4D more accessible and fit for the identified purposes (Section 5)

## 2 THE CONCEPTUAL FRAMEWORK

VLS is the simulation of laser scanning using models of scenes, platforms, scanners, and the beam-scene interaction (Fig. 3; Winiwarter *et al.*, 2022b). While in traditional VLS-3D, the acquisition has always been dynamic, supporting mobile platforms, the virtual landscape (scene) has been static. With the term 'dynamic' in the VLS-4D framework, we specifically refer to the input scene. The scene model is a small and simplified section of the real or a fictional world. In VLS-4D, scene objects can undergo any changes that are relevant to the simulated ray-scene interaction, specifically changes to geometric or material properties. Geometric changes of objects in a scene can be categorised as rigid body displacement, deformation, or as the complete replacement, removal, or addition of objects. Material changes typically refer to changes in the spectral properties. Scene changes may occur between several acquisitions (epochs), between scans or flight strips of a single acquisition, or during a single scan (Fig. 5). We will give an overview of vegetation dynamics that can be observed with LiDAR and reproduced in VLS-4D (Section 2.1). Based on this, we will discuss three change logic concepts for VLS-4D and explain for which combinations of vegetation dynamics and LiDAR acquisition scenarios they are suitable (Section 2.2).

### 2.1 Vegetation dynamics observable with LiDAR

The use of VLS-4D requires data or knowledge about the dynamics of the object to be replicated and virtually observed. In this section, we discuss vegetation dynamics that can be observed with LiDAR, which are summarised in Fig. 4. These dynamics

107 occur at different temporal and spatial scales, which often overlap. Plants move during the day related to water status or wind,  
 108 change during the phenological cycle, and grow taller during their lifetime. In addition to geometric changes, plants also change  
 109 in material properties, e.g., as a result of chlorophyll degradation. Many studies have shown that vegetation dynamics can be  
 110 uncovered with laser scanning. Geometric and backscatter information from laser scanning point clouds have been used to  
 111 investigate tree sway [Vaaja et al., 2016; Yun et al., 2025], diurnal branch and leaf movement [Herrero-Huerta et al., 2018;  
 112 Puttonen et al., 2019; Wang et al., 2022], phenological changes [Bienert et al., 2024; Calders et al., 2015; Shcherbacheva et al.,  
 113 2024], stress-induced changes [Jacobs et al., 2022; Junttila et al., 2019], as well as growth and biomass dynamics [Tompalski  
 114 et al., 2021; Zhao et al., 2018]. Most of these studies rely on multi- or hyper-temporal datasets to quantify changes occurring  
 115 during days, months, or years. In case of wind-induced vegetation movement, effects are visible in individual mono-temporal  
 116 point clouds (Figs 2 and 4).

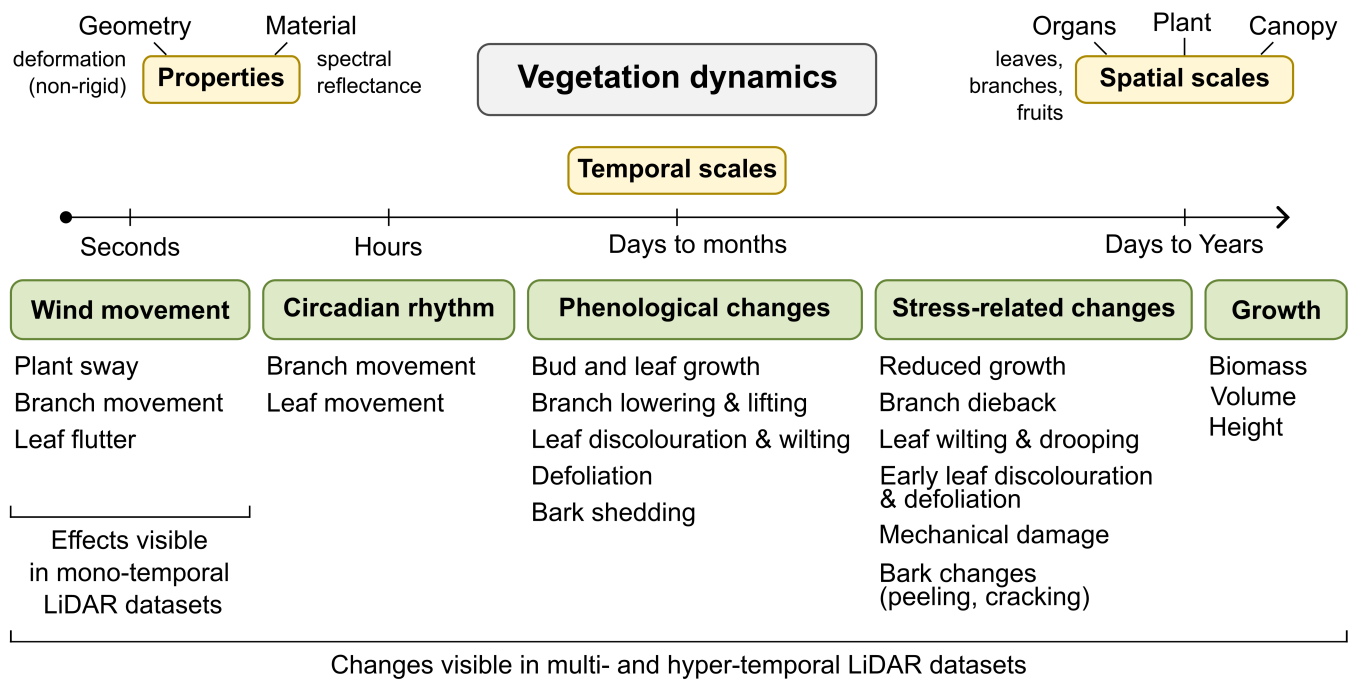


Figure 4: Overview of vegetation dynamics that can be observed with LiDAR and have been described in the literature. Changes can affect geometric and material properties, and often occur simultaneously at overlapping spatial and temporal scales (yellow boxes). Examples of vegetation dynamics are listed, grouped by their drivers and temporal scales (green boxes). Wind-induced motion can affect single acquisitions, whereas dynamics over longer time scales are only visible between epochs.

117 For most of these vegetation dynamics, reference data is difficult to collect in the real world. This is why we propose the simula-  
 118 tion of LiDAR surveys in virtual scenes with defined geometric, material and dynamic properties (VLS-4D) as a complementary  
 119 approach to generate point clouds with (virtual) 'ground truth'. To ensure fitness for purpose, VLS-4D must be implemented  
 120 using use case-specific approaches (Sections 2.2 and 3).

121 2.2 Scene change logic

122 In order to implement the vegetation changes described in Section 2.1, we propose three main concepts and illustrate them with  
 123 examples (Fig. 5).

124 2.2.1 Concept of one static snapshot per epoch

125 Monitoring dynamics such as forest growth [Tompalski et al., 2021] or tree phenology [Wittke et al., 2024] requires multi-  
 126 hyper-temporal LiDAR datasets, as acquired by repeated Airborne Laser Scanning (ALS) or permanent TLS. These datasets can  
 127 be simulated using an updated static scene snapshot, assuming that minor changes during individual acquisitions, such as tree  
 128 movement caused by wind, can be neglected. This can be justified either by the spatial resolution being too low to register such  
 129 changes or by their magnitude being insignificant relative to the changes between epochs. In this approach, the scene remains  
 130 unchanged during a single simulation run and the simulation is repeated across different versions of a scene to capture changes  
 131 over time (Fig. 5a).

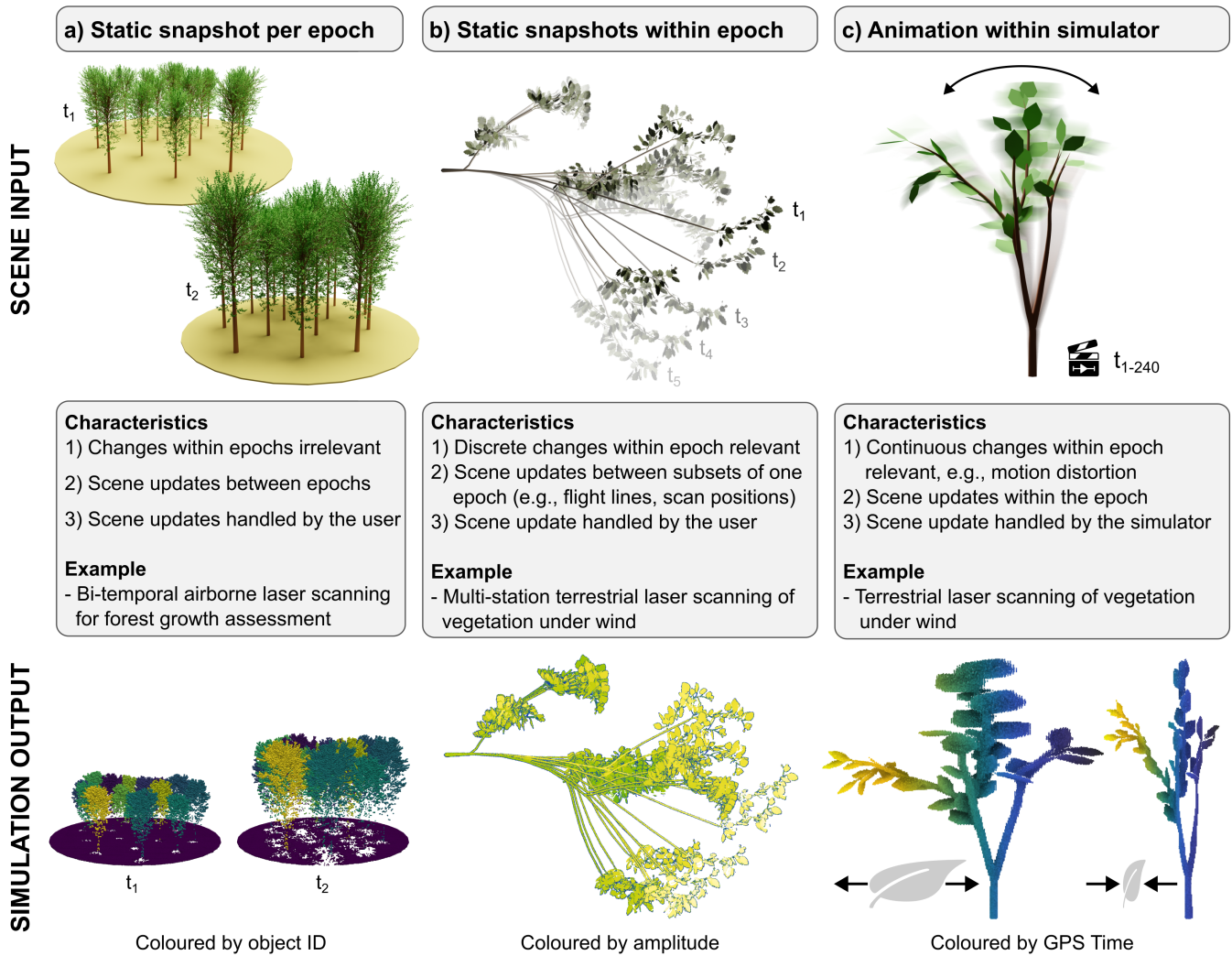


Figure 5: Overview of the three change logic concepts. The first row shows exemplary dynamic input scenes, the second row names the characteristics of each concept and suitable VLS-4D scenarios, and the bottom row shows exemplary VLS-4D point clouds, simulated with HELIOS++ v2.0.2.

### 132 2.2.2 *Concept of several static snapshots within an epoch*

133 We propose the second concept to study effects from wind-induced vegetation movement between individual flight lines of an  
134 ALS campaign or between individual scan positions of a multi-station TLS survey. In this concept, several static scene snapshots  
135 are created for one epoch and used to simulate different subsets (i.e., flight lines or scan positions) of a survey.

136 In the example of multi-station TLS, using an updated scene snapshot for each scan position enables recreating duplication effects,  
137 where branches appear in different positions across scans (Figs 2b and 5b). Snapshots may be sampled from a 3D animation of a  
138 tree swaying in the wind. With this approach, both windless and wind-affected point clouds can be generated for the same plant,  
139 which would require controlled lab experiments in the real world.

### 140 2.2.3 *Concept of animation within the simulator*

141 The third concept is essential for simulating movement effects within a single scan, such as a branch being displaced by a gust of  
142 wind, which leads to point cloud distortions (Figs 2a and 5c). In this case, the virtual scene needs to change continuously during  
143 a single simulation run and therefore requires frequent scene updates. This implies that the animation must be integrated into  
144 the simulator (Fig. 5c), where the simulation engine manages scene updates automatically based on the definition of the dynamic  
145 scene behaviour and the update frequency.

146 The aforementioned theoretical considerations of scene dynamics in LiDAR simulation require methods for animating vegetation  
147 scenes, as well as support for such animations in existing LiDAR simulation software. These aspects will be addressed in the  
148 next section.

## 149 3 HOW VLS-4D CAN BE IMPLEMENTED

150 To perform VLS, you need three fundamental steps: 1) the generation of a 3D scene, 2) the configuration of the scanner, platform  
151 behaviour and survey settings, and 3) the execution of the survey (Fig. 3). In VLS-4D, we must either model multiple versions  
152 of the scene that represent different points in time or create 3D animations. While repeated surveys with static snapshot scenes  
153 can be processed in any LiDAR simulator, some software also explicitly supports dynamic scenes.

154 In the following, we first give an overview of algorithms for modelling dynamic vegetation (Section 3.1) and then review LiDAR  
155 simulation software solutions for vegetation applications and their compatibility with dynamic scenes (Section 3.2).

### 156 3.1 *Scene generation*

157 We start this section by introducing approaches for automatically generating individual plants. We then present methods for  
158 transforming static tree models into animated ones, and finally review approaches for generating entire dynamic ecosystems.

#### 159 3.1.1 *Data-driven and procedural modelling*

160 The two primary approaches for generating virtual plant models for VLS scenes are data-driven and procedural modelling. Data-  
161 driven modelling refers to the reconstruction of 3D tree models from real-world data, which allows generating digital copies of

162 trees which exist in the real world. Procedural modelling refers to the (semi)automatic generation of 3D models by means of a  
 163 procedure or a program [Smelik et al., 2014], enabling the generation of large and structurally diverse datasets.

Table 1: Approaches for 3D modelling of individual trees by reconstruction from 2D or 3D data.

Input	Output	Examples
Tree point cloud	Voxel model	Li et al. [2024]; Schäfer et al. [2023]; Weiser et al. [2021]
Tree point cloud	Polygonal 3D tree model	AdTree [Du et al., 2019] SimpleForest [Hackenberg et al., 2021] TreeQSM [Raumonen et al., 2013]
Tree image	Polygonal 3D tree model	Deep learning-based [Li et al., 2021a] Image-guided non-parametric tree growing [Tan et al., 2008]

164 In data-driven modelling, 3D tree models are typically reconstructed from 3D point clouds but also 2D images (Table 1). This  
 165 approach is the basis for creating digital twins. A key advantage is that dynamics derived from real-world data can be incorporated  
 166 into the digital model. Using point clouds for reconstruction also allows the assessment of realism by comparing simulated point  
 167 clouds with their real-world counterparts. Several studies employing static-scene VLS or radiative transfer modelling have  
 168 utilised tree models created from real-world point cloud data, in the form of cylinder models [Calders et al., 2018; Esmorís et al.,  
 169 2024; Stocker et al., 2023] or voxel models [Schäfer et al., 2023; Li et al., 2024]. Detailed cylinder models are essential for  
 170 simulating close-range acquisitions, e.g., TLS, and for applications requiring precise branching structure or individual leaves,  
 171 such as leaf-wood separation. These models demand high-resolution input data, typically from TLS. In contrast, voxel models  
 172 are more suitable for ALS and UAV-based Laser Scanning (ULS) simulations. They should be reconstructed from point clouds  
 173 of much higher resolution or quality than those to be simulated [Weiser et al., 2021; Winiwarter et al., 2022a], but are not limited  
 174 to TLS data.

175 The key advantage of procedural modelling is that just a small set of parameters or rules results in a wide variety of complex mod-  
 176 els, a concept that Smith [1984] describes as database amplification. Compared to manual and data-driven modelling, procedural  
 177 techniques significantly reduce the effort to create realistic virtual environments on larger scales. Table 2 lists tree modelling  
 178 software based on procedural modelling that have been used in LiDAR simulation studies, specifying their dynamic features,  
 179 their licence types and selected VLS case studies. Most of the solutions already support dynamics in the form of wind and growth  
 180 animation, which makes them suitable for VLS-4D workflows.

### 181 3.1.2 From static to animated plants

182 Once a static base scene has been created, manual editing can be effective in creating new versions for VLS-4D scenarios:  
 183 Branches can be removed from a tree to simulate branch dieback or pruning, or trees can be scaled, removed, or replaced to  
 184 simulate growth, harvesting, and replanting.

185 Beyond that, several algorithms have been proposed to automatically convert static triangular meshes into animated models  
 186 (Table 3). These animated plant models can be created by deriving motion from point cloud sequences and transferring it onto a  
 187 mesh [Li et al., 2013]. Other approaches aim to generate 'simulation-ready' tree models which, unlike the input polygonal tree  
 188 model, are semantically segmented and hierarchically organised, enabling deformation through physical simulations of wind or

Table 2: Procedural modelling based tree generation software solutions, their support for wind and growth animation, their licence type and VLS case studies where they have been used.

Software	Wind animation	Growth animation	Licence type	Virtual laser scanning case studies
Arbaro	✗	✗	Free & open source	<i>Liu et al. [2019]; Zhu et al. [2020]</i>
Sapling Tree Gen	✓	✗	Free & open source	<i>Albert et al. [2025]; Bornand et al. [2024]</i>
Tree It	✓	✗	Free	<i>Raverta Capua et al. [2025]</i>
OnxyTREE	✓	✓	Commercial	<i>Cai et al. [2024]; Jiang et al. [2021]; Li et al. [2021b]</i>
AmapSim	✓	✓	Free	<i>Lecigne et al. [2021]</i>
xfrog	✓	✓	Commercial	<i>Grau et al. [2017]; Widlowski et al. [2015]</i>
TheGrove	✓	✓	Commercial	<i>Bornand et al. [2024]</i>
SpeedTree	✓	✓	Commercial	<i>Wang et al. [2022]</i>

<https://sourceforge.net/projects/arbaro/>, [Weber and Penn, 1995]

[https://docs.blender.org/manual/en/4.1/addons/add\\_curve/sapling.html](https://docs.blender.org/manual/en/4.1/addons/add_curve/sapling.html), [Weber and Penn, 1995]

<http://www.evolved-software.com/treeit/treeit>

<https://www.onyxtree.com/>

<https://amapstudio.cirad.fr/soft/amapsim/start>, [Barczi et al., 2008]

<https://www.xfrog.com/xfrog-software>, [Lintermann and Deussen, 1999]

<https://www.thegrove3d.com/>

<https://store.speedtree.com/>

URLs last accessed: 2025-02-11.

189 gravity [*Li et al., 2013; Zhao and Barbič, 2013*]. Finally, several studies generate models of developmental stages of trees [*Stava*  
 190 *et al., 2014; Pirk et al., 2012, 2014; Zhou et al., 2024*], which represent tree growth or environmental responses as sequences of  
 191 static models. The static input 3D models of the approaches in Table 3 may be taken from public tree model libraries, generated  
 192 using procedural modelling, or reconstructed from real-world data (Section 3.1.1).

Table 3: Examples of algorithms to turn static 3D tree models or 2D sequences into moving or evolving 3D tree models.

Input	Output	Description	Reference
2D video	Animated tree models	Probabilistic generative modelling and motion tracking	<i>Li et al. [2011]</i>
Static polygonal tree model and real-world captured growth sequences	Animated plant models	Motion and growth transfer	<i>Li et al. [2013]</i>
Static polygonal tree model	Simulation-ready tree models	Hierarchical organ segmentation	<i>Li et al. [2013]</i>
Static polygonal tree model	Simulation-ready plant model	Pre-processing (authoring) pipeline	<i>Zhao and Barbič [2013]</i>
Static polygonal tree model	Parameters of a procedural model	Inverse procedural model	<i>Stava et al. [2014]</i>
Static polygonal tree model	Arbitrary intermediate stages in tree development and animations	Developmental model	<i>Pirk et al. [2012]</i>
Static polygonal tree model, parameters of developmental model and parameters of wind emitter	Developmental stages with immediate and long-term wind response	Wind simulation	<i>Pirk et al. [2014]</i>
Static polygonal tree models (procedural) for training, and global priors (species, age, gravitropism)	Developmental stages (among others)	Iterative deep learning pipeline	<i>Zhou et al. [2024]</i>

### 193 3.1.3 From single plants to dynamic ecosystems

194 The previous approaches have focused on the individual plant level. When we want to perform multi-temporal VLS-4D on the  
195 stand level, e.g., for different scenarios of climate warming or silvicultural management, it is essential to simulate ecosystem  
196 dynamics and account for factors such as vegetation growth, environmental conditions, and competition. Approaches for this can  
197 be drawn from two distinct fields: forestry, which provides empirical or process-based models of forest growth, and computer  
198 graphics, which offers algorithms for generating visually realistic, explicit 3D models.

199 Forest growth models have been widely used for decades as operational tools to support decision making in forestry. These  
200 models help estimate forest growth and yield, predict the impacts of management practices, and study forest dynamics [Porté and  
201 Bartelink, 2002]. FORMIND [Fischer et al., 2016] and TROLL [Chave, 1999], two popular individual tree-based forest growth  
202 models, both have a LiDAR simulation module implemented, which makes them particularly interesting for VLS-4D (Section  
203 3.2). Building on processes implemented in FORMIND, Henniger et al. [2023] presented Forest Factory 2.0, a model to generate  
204 virtual dynamic forest stands for different biomes, which was used in several VLS studies for biomass estimation [Schäfer et al.,  
205 2024; Yu et al., 2024].

206 Ecosystem modelling approaches from computer graphics prioritise visual realism and aesthetics. These approaches usually  
207 include detailed geometric representations of plants, making them well-suited for direct use in LiDAR simulation. Deussen et al.  
208 [1998] present a multilevel modelling and rendering pipeline for plant ecosystems based on procedural modelling. Similarly,  
209 Makowski et al. [2019] present a multi-scale modelling approach to generate ecosystems, which dynamically adapt over time  
210 based on developmental traits, terrain characteristics, and climatic conditions. Another notable contribution is the work of  
211 Pałubicki et al. [2022], which focuses on modelling the climate response of vegetated ecosystems. While the algorithms presented  
212 here and in Section 3.1.2 show great potential to generate input for VLS-4D, they are not available as free software for researchers  
213 in forestry, ecology, and remote sensing (Section 5).

### 214 3.2 LiDAR simulation

215 The aim of LiDAR simulators used in remote sensing and vegetation research is to accurately model the geometric and radiometric  
216 properties of point clouds from survey-grade laser scanners. The input scenes to these simulators have traditionally been static,  
217 neglecting vegetation movement and growth. LiDAR simulators developed in other fields already focus on animated scenes  
218 as they are used for object detection and tracking tasks, e.g., for autonomous driving [Gschwandtner et al., 2011; Reitmann  
219 et al., 2021; Rott, 2022]. However, they implement simplified single-return LiDAR models (with zero beam divergence) that  
220 do not meet the typical requirements of VLS studies for vegetation. Simulation of multiple returns is important for vegetation  
221 applications, as illustrated by the point cloud section shown in Fig. 6. Here, 40% of the returns are intermediate or last returns  
222 that would be missing if beam divergence were neglected.

223 Table 4 lists LiDAR simulators commonly used in applications of remote sensing and vegetation. Regarding the sampling  
224 principle, these simulation frameworks fall into three categories: those based on Monte Carlo ray tracing (MCRT), those based  
225 on deterministic ray tracing, and those based on a simple probabilistic approach. MCRT relies on the statistical convergence  
226 of a large number of simulated rays, allowing it to handle multiple scattering events within the tree crown. This is physically

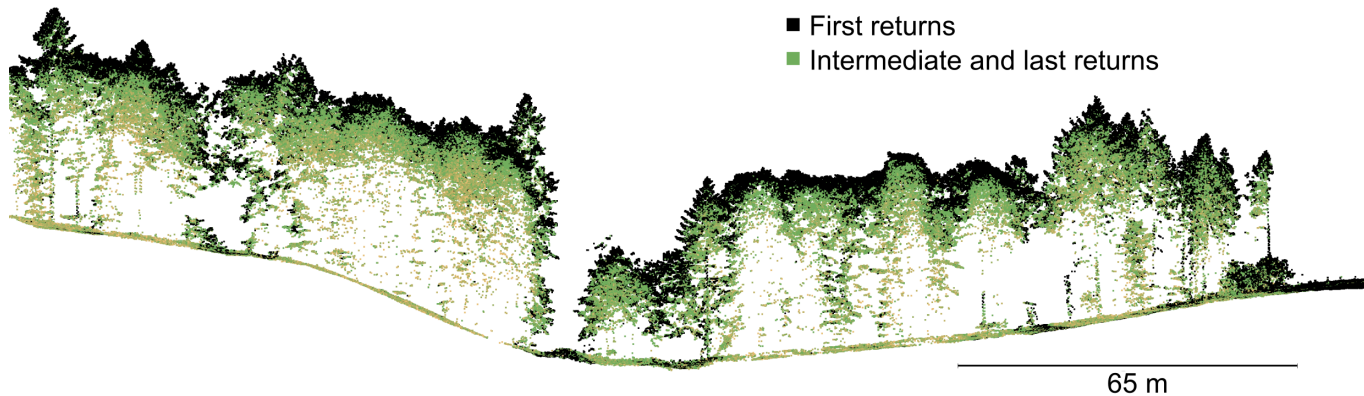


Figure 6: Real-world airborne laser scanning point cloud cross-section coloured by return number (first returns in black). 60% of the points are first returns and 40% are intermediate or last returns.

227 more accurate, but comes at a higher computational cost than deterministic ray tracing, which assumes that light is reflected  
 228 only once before reaching the sensor [Disney et al., 2000; Gastellu-Etchegorry et al., 2016]. Deterministic ray tracing is usually  
 229 sufficient if geometric point cloud features are of primary interest. MCRT-based LiDAR simulators of radiative transfer models  
 230 are recommended for studies where radiometric and full-waveform (FWF) information are required (e.g., to support species  
 231 classification from FWF ALS data; Koenig and Höfle, 2016) or where atmospheric effects should be considered (e.g., spaceborne  
 232 LiDAR). Radiative transfer models like DART are used to simulate a wider range of remote sensing products, enabling the  
 233 simulation of LiDAR point clouds and complementary satellite imagery of the same scene.

234 The simulators in Table 4 support two types of vegetation scenes: i) explicit 3D geometry and ii) primitives filled with turbid  
 235 medium. Explicit geometry is represented as polygonal meshes with individual branches and leaves (cf. Section 3.1). Such  
 236 representations are needed for simulating high-resolution acquisitions and have been used for studies on leaf-wood separation  
 237 [Vicari et al., 2019] or plant movement [Wang et al., 2022]. Different optical properties, e.g., for the bark and the leaves, can  
 238 be defined through material settings. Turbid medium approaches are used for simulations of lower resolution, i.e., airborne  
 239 and spaceborne LiDAR. They use simplified crown shapes and/or voxelised representations. A turbid medium is a statistical  
 240 representation of matter, commonly used to simulate fluids and foliage [Gastellu-Etchegorry et al., 2015]. In radiative transfer  
 241 models, the turbid medium of tree crowns is characterised by the structural parameters leaf area density and leaf angle distribution  
 242 and the optical parameters transmittance and reflectance [Gastellu-Etchegorry et al., 2016; North, 1996]. The turbid medium  
 243 assumption is also the basis for the simple LiDAR sampling approach used by the forest growth models FORMIND and TROLL,  
 244 which calculates probabilities for LiDAR returns in the medium based on the Beer-Lambert law [Knapp et al., 2018; Schmitt  
 245 et al., 2023].

246 Vegetation dynamics of larger scale, such as tree growth, can be represented with both explicit geometry and turbid medium  
 247 approaches. For turbid medium representations, multi-temporal virtual scenes can be parametrised by adjusting properties like  
 248 leaf area density and reflectance [Koetz et al., 2005], as well as scaling the bounding volumes of the medium. The turbid medium-  
 249 based LiDAR simulators of FORMIND and TROLL can automatically generate a point cloud for each time step of the forest  
 250 growth model, enabling the synthetisation of VLS time series of long-term forest dynamics. Fine-scale tree movement - such as  
 251 branch lifting and lowering, tree sway and leaf flutter - are better represented by explicitly modelling individual branches and

Table 4: Overview of commonly used LiDAR simulation software in remote sensing and forest studies. The table details the sampling principle (RT = ray tracing), simulation of beam divergence and full waveforms (FWF), the possible scene object representations, and the supported scene dynamics. It is organised such that LiDAR simulators with similar features are grouped together, facilitating comparison between them.

Name	Sampling principle	Beam div. & FWF	Scene object representation	Scene dynamics	References
FLIGHT	Monte Carlo RT	✓	Turbid medium	✗	<i>North</i> [1996]; <i>North et al.</i> [2010]
librat	Monte Carlo RT	✓	Explicit geometry, turbid medium	✗	<i>Lewis</i> [1999]
DART LiDAR	Quasi-Monte Carlo RT	✓	Explicit geometry, turbid medium	✗	<i>Gastellu-Etchegorry et al.</i> [2015, 2016]
LESS LiDAR	Deterministic RT	✓	Explicit geometry	✗	<i>Qi et al.</i> [2019]; <i>Luo et al.</i> [2023]
HELIOS++	Deterministic RT	✓	Explicit geometry, turbid medium	Rigid motions	<i>Winiwarter et al.</i> [2022b]
FORMIND LiDAR	Simple probabilistic approach based on Beer-Lambert law	✗	Turbid medium	Forest growth	<i>Knapp et al.</i> [2018]
TROLL LiDAR		✗			<i>Schmitt et al.</i> [2023]

<https://flight-rtm.github.io/index.html>

<https://github.com/profLewis/librat>

<https://dart.omp.eu/#/>

<http://lessrt.org/>

<https://github.com/3dgeo-heidelberg/helios>

<https://formind.org/>

<https://github.com/TROLL-code/TROLL>, <https://github.com/sylvainschmitt/rcontroll>

URLs last accessed: 2025-02-11.

252 leaves. These detailed scenes can then be animated to simulate dynamics within a single simulation (Section 2.2.3). While all  
 253 LiDAR simulators in Table 4 can be used in the VLS-4D concepts of static snapshots (Section 2.2), only HELIOS++ explicitly  
 254 supports object dynamics during a single scan, but only rigid motions (as of version 2.0). For VLS-4D of vegetation, we can learn  
 255 from other established LiDAR simulation tools that incorporate dynamic scene capabilities, such as those built into 3D modelling  
 256 and robotics software (Section 5).

## 257 4 WHERE VLS-4D CAN MAKE AN IMPACT: APPLICATIONS IN VEGETATION MONITORING

258 In this section, we review previous studies using VLS-4D, extending beyond ecological applications, and propose further research  
 259 directions for vegetation monitoring. We group the applications into three main methodological categories:

- 260 1. Investigating effects from LiDAR data acquisition and vegetation movement
- 261 2. Developing and evaluating new methods for vegetation change detection and analysis
- 262 3. Generating training and test data for supervised machine learning

### 263 4.1 LiDAR data acquisition and vegetation movement effects

264 Wind-induced vegetation movement can have a significant effect on LiDAR point clouds. This has been reported as a quality issue  
 265 not only in TLS data [*Liang et al.*, 2022; *Vaaja et al.*, 2016], but also for strip alignment in ALS and ULS data [*Sun et al.*, 2023].

266 VLS serves as a valuable tool for investigating how the laser beam interacts with the scene and how vegetation is represented  
267 in the LiDAR point clouds, depending on the acquisition settings and vegetation dynamics. Unlike in real-world experiments,  
268 individual effects can be isolated and controlled, and reference data on the objects and their dynamics is available.

269 VLS-4D can help to better understand the distortion and duplication effects that can be observed in single-epoch TLS point  
270 clouds (Fig. 2; [Medic et al., 2023](#)). [Weiser \[2024\]](#) and [Albert et al. \[2025\]](#) investigated how wind-induced tree movement during  
271 multi-station TLS affects the accuracy of point cloud-derived metrics and the performance of ML-based leaf-wood classification.  
272 They generated wind-affected simulated point clouds by virtually scanning an updated version of a tree from each position. This  
273 knowledge of wind effects can be used to develop algorithms to correct for such motion effects or to quantify and interpret motion  
274 to better understand plant dynamics ([Medic et al., 2023](#); Sections 4.2 and 4.3). Assessing the effects of vegetation movement on  
275 point cloud occlusion could be another research direction for VLS-4D.

276 Researchers can leverage VLS-4D to optimise data acquisition strategies. Using static scenes, [Li et al. \[2021b\]](#) have developed  
277 an iterative-mode scan design based on LiDAR simulation of virtual forest plots of different structure and complexity. Their  
278 proposed scan design aims to minimise occlusion effects and resulting errors in tree parameters. Such analysis could be extended  
279 to forest plots with tree sway, to optimise the acquisition design not only for completeness of coverage but also for mitigation of  
280 wind effects. For a geomorphological application, [Winiwarter et al. \[2022a\]](#) performed VLS-4D to investigate the detectability of  
281 rill erosion in ALS point cloud time series acquired at different flight altitudes. A similar study design could be adapted to forest  
282 mensuration. VLS-4D could also be used to find optimal LiDAR acquisition intervals to pinpoint the timing of leaf emergence  
283 and senescence, to study how these phenological events are affected by climate warming.

284 Simulation can also be used to experiment with sensors, and even allows implementing hypothetical specifications that sensors  
285 on the current market do not support. Using LESS [[Luo et al., 2023](#)], [Zhao et al. \[2023\]](#) conducted a simulation study to assess  
286 the suitability of a prototype airborne hyperspectral LiDAR sensor for monitoring forest insect and disease stress. Their scenarios  
287 included different stages and locations of leaf damage, expressed by leaf spectra measured from real leaves at different levels of  
288 damage.

#### 289 4.2 Method development for change detection and analysis

290 VLS-4D is a valuable tool for validating change analysis and change detection methods as it provides virtual 'ground truth' data  
291 on the states of the scene objects at each epoch. As demonstrated in previous static scenario VLS case studies, it is considered  
292 best practice to evaluate the performance of a novel method on both synthetic and real data (e.g., [Liu et al., 2022](#); [Vicari et al.,](#)  
293 [2019](#); [Wu et al., 2021](#)). Synthetic data, with its inherent reference data, enables quantitative evaluation across arbitrary scenarios  
294 but suffers from a sim-to-real domain gap. Real-world data is therefore essential to confirm effectiveness, though evaluations are  
295 often limited to small datasets, specific scenarios, or qualitative assessments.

296 Recognising wind-induced plant movement as a source of uncertainty or error in point cloud measurements (Section 4.1), methods  
297 are needed to reliably mitigate wind effects. For the case of duplication of plant organs (Fig. 2b), this can be achieved with  
298 additional non-rigid registration [[Medic et al., 2023](#); [Wang et al., 2022](#)] after conventional rigid point cloud registration. Non-  
299 rigid registration aims to align multiple point clouds while accounting for changes in plant shape. [Wang et al. \[2022\]](#) employed bi-

300 temporal VLS to validate PlantMove, a tool for quantifying plant movement via coarse-to-fine non-rigid point cloud registration.  
301 They used a SpeedTree-generated tree model and created two static representations - before and after applying a non-linear  
302 transformation function. These were then scanned in two epochs, and the PlantMove motion fields compared with the known  
303 simulated motion fields. [Wang et al. \[2022\]](#) also demonstrated their method on real-world datasets, for which they however lacked  
304 accurate and full-coverage reference displacement values.

305 VLS-4D can also generate time series of sequential point clouds, which can be used to develop algorithms for change analysis  
306 [[Winiwarter et al., 2022a](#)]. As introduced in Section 1 (Fig. 1), monitoring plant growth and health can often be complicated by  
307 the use of different sensor systems and acquisition setups over time. Here, VLS-4D provides the option to perform multi-temporal  
308 LiDAR simulations from different sensors and to include not only changes of interest (e.g., tree growth), but also other changes  
309 (e.g., wind movement, seasonal changes). This enables the development of methods that are targeted at specific changes and  
310 robust to change noise and inconsistent measurement scenarios. Future methods developed with the support of VLS-4D may  
311 even be able to disentangle signals from different change processes, e.g., wind sway and tree growth.

### 312 4.3 Training data generation

313 There are two main motivations for generating training data using VLS-4D. First, VLS-4D generates sequential data that is  
314 essential for change-related tasks, such as change detection, object tracking, or scan registration. Second, VLS-4D can be used  
315 to create so much variability in the simulated training data that the model can generalise to real-world data, a concept known as  
316 domain randomisation [[Tobin et al., 2017](#)].

317 Simulated LiDAR training data has been exploited for various ML and deep learning (DL) applications in forestry and ecology  
318 such as tree instance segmentation [[Wang, 2020](#); [Liu et al., 2025](#)], semantic segmentation [[Cai et al., 2024](#); [Wang, 2020](#); [Esmoris  
319 et al., 2024](#); [Liu et al., 2025](#); [Stocker et al., 2023](#)] or biomass estimation [[Schäfer et al., 2024](#)], but these studies have only used  
320 static scenarios. In other domains, VLS-4D training data have already been used successfully for change analysis. [de Gélis et al.  
321 \[2023\]](#) and [Zahs et al. \[2023\]](#) used bi-temporal VLS-4D training data for urban change analysis and building damage assessment,  
322 respectively. [de Gélis et al. \[2023\]](#) show that pre-training with their simulated point cloud dataset significantly reduces the  
323 amount of labelled data samples needed in the fine-tuning step on real data. In computer vision, sequential point cloud datasets  
324 have been simulated from animations of humanoids and animals [[Huang et al., 2023](#); [Li and Harada, 2022](#)]. These VLS-4D  
325 datasets are used to train and validate DL methods for non-rigid point cloud registration (Section 4.2). Such existing methods  
326 may be directly applied to multi-station TLS point clouds with vegetation wind effects, allowing windless representations to be  
327 computed. However, fine-tuning with targeted and domain-specific VLS-4D training and validation data of moving plants might  
328 further improve the results [[Medic et al., 2023](#)] and we see this as a future research direction.

329 [Knapp et al. \[2018\]](#) used VLS-4D in conjunction with the forest growth model FORMIND to simulate a wide range of succes-  
330 sional stages of a tropical rainforest under different disturbance regimes. This generated large amounts of simulated LiDAR  
331 data with corresponding inventory data. By further varying LiDAR acquisition settings, the approach could serve as domain ran-  
332 domisation, enabling effective training of DL-based biomass models. Virtual LiDAR time series based on forest growth models  
333 could also be employed to train models for quantifying forest succession, growth, and the impacts of disturbances. Models for  
334 assessing forest pests and diseases benefit from the combination of LiDAR metrics and hyperspectral metrics as predictors [[Stone](#)

335 *and Mohammed, 2017*]. Hybrid (point cloud and image) multi-temporal datasets (e.g., *Zhao et al., 2023*) can be generated by  
336 radiative transfer models such as DART or LESS, which can simulate both LiDAR data and multi- and hyperspectral imagery of  
337 the same synthetic scenes.

338 In general, there is still little literature on Artificial Intelligence (AI) for change detection at the point level [*de Gélis et al.,*  
339 *2024*] and even less so for vegetation change detection. Reasons for this include a) the lack of open multi-temporal point clouds  
340 datasets and b) the difficulty of relating multi-temporal point cloud features to change signals due to the lack of reference data.  
341 With the current developments in sensing systems and AI, we expect more algorithms to be developed in the near future. Here,  
342 VLS-4D can be a means of accelerating methodological progress, complementing real-world benchmark datasets. VLS-4D can  
343 significantly enhance the volume, diversity and labelling quality of point cloud training datasets for vegetation change analysis,  
344 while also speeding up data provisioning.

## 345 5 OPEN CHALLENGES

### 346 5.1 Closing the implementation gap of VLS-4D of vegetation

347 To date, there are only a few studies using VLS-4D to investigate vegetation dynamics [*Wang et al., 2022; Albert et al., 2025*] or  
348 other environmental processes. Besides the aspect of realism (Section 5.2), this is due to the limited accessibility of automated  
349 algorithms for dynamic scene generation and the limitations of current LiDAR simulation frameworks.

350 Regarding dynamic scene generation, we found that the software that can animate tree movement and growth with high geometric  
351 and dynamic realism is primarily commercial (Table 2). In addition to the potentially prohibitive cost of acquiring the software,  
352 software licences may also prohibit the sharing of generated 3D models and animations, which is contrary to many of the open  
353 data efforts currently practiced in the forestry community (e.g., *Ouaknine et al., 2025; Puliti et al., 2025*). In the fields of computer  
354 graphics, simulation, and animation, many technical solutions for creating dynamic vegetation scenes already exist, using real-  
355 data or procedural models, and from individual plants to entire ecosystems (Section 3.1). However, these methods are often not  
356 freely available. The remote sensing community would benefit from greater accessibility in the form of open-source software to  
357 reduce the effort required to create dynamic scenes.

358 Regarding simulation frameworks, there is currently no solution that combines sophisticated and realistic laser beam modelling  
359 (i.e., beam divergence, full waveforms) with support for arbitrary animations within the simulator (Section 3.2). In VLS-4D  
360 frameworks integrated with 3D modelling or robotics software, complex animations (e.g., skeleton animation and physics-based  
361 simulation) are possible, but scan patterns, LiDAR intensity computations and noise models are simplified, and beam divergence  
362 is completely neglected, which is problematic for vegetation applications. Nevertheless, these frameworks can serve as valuable  
363 templates and facilitate the further development of vegetation-oriented LiDAR simulators through knowledge and technology  
364 transfer.

### 365 5.2 Assessing and enhancing realism

366 The biggest challenge in VLS-4D remains the same as for VLS of static scenes: the reality gap between real and simulated  
367 data. On the one hand, VLS-4D can be a means to close this gap, since in many cases, neglecting scene dynamics results

368 in unrealistic simplification of real scenes. On the other hand, VLS-4D adds additional complexity to VLS by including the  
369 temporal dimension. In addition to conventional VLS components - such as scene geometries, material properties, scan patterns,  
370 beam divergence, multiple returns, and sensor noise - VLS-4D requires realistic modelling of the type, speed and resolution of  
371 scene dynamics. If the dynamics are not modelled in a suitable way, VLS-4D point clouds may be even less realistic than their  
372 conventional VLS-3D counterparts. Further work is required to develop approaches and metrics for thoroughly analysing the  
373 realism and fitness for purpose of the simulated data (e.g. [Manivasagam et al., 2023](#)). This highlights the need for accessible  
374 algorithms to generate animated models of real-world plants, enabling direct comparisons between real and simulated point  
375 clouds under controlled conditions. Such analyses can then identify the most effective adjustments to enhance the realism of  
376 simulations.

377 Several ML and DL studies have shown that there is a consistent performance gap between models trained on real data and models  
378 trained on simulated VLS data alone [[Liu et al., 2025](#); [Schäfer et al., 2023](#)]. Considering this reality gap, we recommend the use  
379 of labelled simulated training data in three key ways: (1) in hybrid models trained on a small set of real data complemented by  
380 large amounts of simulated data [[de Melo et al., 2022](#); [Liu et al., 2025](#)], (2) for pre-training DL models, which are later fine-tuned  
381 on real-world data [[Liu et al., 2025](#)], and (3) by applying domain adaptation techniques [[Bryson et al., 2024](#); [de Melo et al., 2022](#)].  
382 Since the dynamics implemented in digital twins for VLS-4D shall closely resemble the real-world dynamics, good knowledge of  
383 vegetation processes is essential to ensure sufficient realism. To parametrise virtual scenes, VLS-4D benefits from basic research  
384 on vegetation dynamics, including tree phenology and tree sway, as quantified using numerical simulations [[Zanotto et al., 2024](#)],  
385 complementary sensors such as accelerometers and strain gauges [[Jackson et al., 2021](#); [Jaeger et al., 2022](#)] or cameras [[Gibbs  
386 et al., 2019](#); [Kattenborn et al., 2022](#)].

## 387 6 CONCLUSION

388 Vegetation dynamics clearly affect mono- and multi-temporal LiDAR representations. The integration of vegetation dynamics  
389 into VLS therefore has significant potential to advance LiDAR-based vegetation monitoring, particularly in the context of multi-  
390 temporal and multi-sensor data analysis and the growing need for labelled training data for DL approaches. Our review highlights  
391 three key areas where VLS-4D can make a difference: (1) investigating LiDAR data acquisition and vegetation movement effects,  
392 (2) supporting the development of new methods for vegetation change analysis, and (3) generating training data for DL. Applica-  
393 tions for VLS-4D can be primarily found in the study of vegetation movement and point cloud quality, the optimisation of data  
394 acquisition, and the monitoring of vegetation growth and health.

395 The concept of approximating dynamic scenes as a series of static representations is fully compatible with the current state-of-  
396 the-art high-fidelity LiDAR simulators used in forestry. In contrast, the direct support of animated virtual scenes remains an area  
397 for future innovation. To fully realize the potential of VLS-4D, increased availability of open-source tools to generate realistic  
398 large-scale dynamic vegetation scenes will be crucial.

399 VLS-4D will be a transformative tool for vegetation research, serving training data generation and method validation where real  
400 data is scarce or suitable reference measurements cannot be obtained. If fitness for purpose is ensured, this framework promises

401 to improve our understanding of LiDAR representations of dynamic vegetation and to support more effective environmental  
402 monitoring and management.

#### 403 ACKNOWLEDGEMENTS

404 This research was funded by the Deutsche Forschungsgemeinschaft (DFG, German Research Foundation) – no. 496418931  
405 (VirtuaLearn3D) and no. 528521476 (Fostering a community-driven and sustainable HELIOS++ scientific software) – and by  
406 the Federal Ministry of Education and Research (BMBF) – no. 02WDG1696 (AIMon 5.0) – within the funding measure "Digital  
407 GreenTech Environmental Engineering meets Digitalisation" as part of the "Research for Sustainability" (FONA) Strategy.  
408 Some of the figures have been designed using resources from Flaticon.com: Figs 2 and 5: Leaf icon by PixelPerfect; Fig. 3:  
409 drone and tripod icons by Freepik, plane icon by Iconjam, configuration icon by RaftelDesig; Fig. 5: animation icon by  
410 gravisio.  
411 Fig. 3 shows a scene rendered in Blender with an airplane model CC-BY Emmanuel Beranger, a house model by free3d.com user  
412 gerald3d, and a drone model by cgtrader.com user CGaxr.

#### 413 CONFLICT OF INTEREST

414 The authors declare no conflict of interest in relation to this paper.

#### 415 REFERENCES

- 416 Albert, W., H. Weiser, R. Tabernig, and B. Höfle, Wind during terrestrial laser scanning of trees: Simulation-based assessment of  
417 effects on point cloud features and leaf-wood classification, *ISPRS Annals of the Photogrammetry, Remote Sensing and Spatial*  
418 *Information Sciences*, in Press, 2025.
- 419 Barczi, J.-F., H. Rey, Y. Caraglio, P. de Reffye, D. Barthélémy, Q. X. Dong, and T. Fourcaud, AmapSim: a structural whole-plant  
420 simulator based on botanical knowledge and designed to host external functional models, *Annals of botany*, 101(8), 1125–1138,  
421 doi:<https://doi.org/10.1093/aob/mcm194>, 2008.
- 422 Bienert, A., K. Richter, S. Boehme, and H.-G. Maas, Investigating the Potential of Hyper-Temporal Terrestrial Laser Point Clouds  
423 for Monitoring Deciduous Tree Growth, *The International Archives of the Photogrammetry, Remote Sensing and Spatial*  
424 *Information Sciences*, XLVIII-2-2024, 33–40, doi:<https://doi.org/10.5194/isprs-archives-XLVIII-2-2024-33-2024>, 2024.
- 425 Bornand, A., M. Abegg, F. Morsdorf, and N. Rehus, Completing 3D point clouds of individual trees using deep learning,  
426 *Methods in Ecology and Evolution*, 15(11), 2010–2023, doi:<https://doi.org/10.1111/2041-210X.14412>, 2024.
- 427 Bryson, M., A. Ravendran, C. Mercier, T. Frickey, S. Jayathunga, G. Pearse, and R. J. Hartley, Domain adaptation of deep neural  
428 networks for tree part segmentation using synthetic forest trees, *ISPRS Open Journal of Photogrammetry and Remote Sensing*,  
429 14, 100,078, doi:<https://doi.org/10.1016/j.ophoto.2024.100078>, 2024.
- 430 Cai, S., W. Zhang, S. Zhang, S. Yu, and X. Liang, Branch architecture quantification of large-scale coniferous forest plots using  
431 UAV-LiDAR data, *Remote Sensing of Environment*, 306, 114,121, doi:<https://doi.org/10.1016/j.rse.2024.114121>, 2024.

- 432 Calders, K., P. Lewis, M. Disney, J. Verbesselt, and M. Herold, Investigating assumptions of crown archetypes for modelling  
433 lidar returns, *Remote Sensing of Environment*, 134, 39–49, doi:<https://doi.org/10.1016/j.rse.2013.02.018>, 2013.
- 434 Calders, K., T. Schenkels, H. Bartholomeus, J. Armston, J. Verbesselt, and M. Herold, Monitoring spring phenology  
435 with high temporal resolution terrestrial LiDAR measurements, *Agricultural and Forest Meteorology*, 203, 158–168,  
436 doi:<https://doi.org/10.1016/j.agrformet.2015.01.009>, 2015.
- 437 Calders, K., N. Origo, A. Burt, M. Disney, J. Nightingale, P. Raunonen, M. Åkerblom, Y. Malhi, and P. Lewis, Re-  
438 alistic forest stand reconstruction from terrestrial LiDAR for radiative transfer modelling, *Remote Sensing*, 10(6), 933,  
439 doi:<https://doi.org/10.3390/rs10060933>, 2018.
- 440 Chave, J., Study of structural, successional and spatial patterns in tropical rain forests using TROLL, a spatially explicit forest  
441 model, *Ecological Modelling*, 124(2-3), 233–254, doi:[https://doi.org/10.1016/S0304-3800\(99\)00171-4](https://doi.org/10.1016/S0304-3800(99)00171-4), 1999.
- 442 Coops, N. C., A. Varhola, C. W. Bater, P. Teti, S. Boon, N. Goodwin, and M. Weiler, Assessing differences in tree  
443 and stand structure following beetle infestation using lidar data, *Canadian Journal of Remote Sensing*, 35(6), 497–508,  
444 doi:<https://doi.org/10.5589/m10-005>, 2009.
- 445 de Gélis, I., S. Saha, M. Shahzad, T. Corpetti, S. Lefèvre, and X. X. Zhu, Deep unsupervised learning for 3D  
446 ALS point clouds change detection, *ISPRS Open Journal of Photogrammetry and Remote Sensing*, 9, 100,044,  
447 doi:<https://doi.org/10.1016/j.ophoto.2023.100044>, 2023.
- 448 de Gélis, I., T. Corpetti, and S. Lefèvre, Change Detection Needs Change Information: Improving Deep 3-D Point Cloud Change  
449 Detection, *IEEE Transactions on Geoscience and Remote Sensing*, 62, 1–10, doi:<https://doi.org/10.1109/TGRS.2024.3359484>,  
450 2024.
- 451 de Melo, C. M., A. Torralba, L. Guibas, J. DiCarlo, R. Chellappa, and J. Hodgins, Next-generation deep learning based on  
452 simulators and synthetic data, *Trends in cognitive sciences*, 26(2), 174–187, doi:<https://doi.org/10.1016/j.tics.2021.11.008>,  
453 2022.
- 454 Deussen, O., P. Hanrahan, B. Lintermann, R. Měch, M. Pharr, and P. Prusinkiewicz, Realistic modeling and rendering of plant  
455 ecosystems, in *Proceedings of the 25th Annual Conference on Computer Graphics and Interactive Techniques*, SIGGRAPH  
456 '98, pp. 275–286, ACM, New York, NY, USA, doi:<https://doi.org/10.1145/280814.280898>, 1998.
- 457 Disney, M., P. Lewis, and P. R. J. North, Monte Carlo ray tracing in optical canopy reflectance modelling, *Remote Sensing*  
458 *Reviews*, 18(2-4), 163–196, doi:<https://doi.org/10.1080/02757250009532389>, 2000.
- 459 Disney, M., V. Kalogirou, P. Lewis, A. Prieto-Blanco, S. Hancock, and M. Pfeifer, Simulating the impact of discrete-return  
460 lidar system and survey characteristics over young conifer and broadleaf forests, *Remote Sensing of Environment*, 114(7),  
461 1546–1560, doi:<https://doi.org/10.1016/j.rse.2010.02.009>, 2010.
- 462 Du, S., R. Lindenbergh, H. Ledoux, J. Stoter, and L. Nan, AdTree: Accurate, detailed, and automatic modelling of laser-scanned  
463 trees, *Remote Sensing*, 11(18), 2074, doi:<https://doi.org/10.3390/rs11182074>, 2019.
- 464 Esmorís, A. M., H. Weiser, L. Winiwarter, J. C. Cabaleiro, and B. Höfle, Deep learning with simulated laser scan-  
465 ning data for 3D point cloud classification, *ISPRS Journal of Photogrammetry and Remote Sensing*, 215, 192–213,  
466 doi:<https://doi.org/10.1016/j.isprsjprs.2024.06.018>, 2024.

- 467 Fischer, R., et al., Lessons learned from applying a forest gap model to understand ecosystem and carbon dynamics of complex  
468 tropical forests, *Ecological Modelling*, 326, 124–133, doi:<https://doi.org/10.1016/j.ecolmodel.2015.11.018>, 2016.
- 469 Gastellu-Etchegorry, J.-P., T. Yin, N. Lauret, E. Grau, J. Rubio, B. D. Cook, D. C. Morton, and G. Sun, Simulation of satellite,  
470 airborne and terrestrial LiDAR with DART (I): Waveform simulation with quasi-monte carlo ray tracing, *Remote Sensing of  
471 Environment*, 184, 418–435, doi:<https://doi.org/10.1016/j.rse.2016.07.010>, 2016.
- 472 Gastellu-Etchegorry, J.-P., et al., Discrete anisotropic radiative transfer (DART 5) for modeling airborne and satel-  
473 lite spectroradiometer and LIDAR acquisitions of natural and urban landscapes, *Remote Sensing*, 7(2), 1667–1701,  
474 doi:<https://doi.org/10.3390/rs70201667>, 2015.
- 475 Gibbs, J. A., A. J. Burgess, M. P. Pound, T. P. Pridmore, and E. H. Murchie, Recovering Wind-Induced Plant Mo-  
476 tion in Dense Field Environments via Deep Learning and Multiple Object Tracking, *Plant physiology*, 181(1), 28–42,  
477 doi:<https://doi.org/10.1104/pp.19.00141>, 2019.
- 478 Grau, E., S. Durrieu, R. Fournier, J.-P. Gastellu-Etchegorry, and T. Yin, Estimation of 3D vegetation density with terrestrial laser  
479 scanning data using voxels. a sensitivity analysis of influencing parameters, *Remote Sensing of Environment*, 191, 373–388,  
480 doi:<https://doi.org/10.1016/j.rse.2017.01.032>, 2017.
- 481 Gschwandtner, M., R. Kwitt, A. Uhl, and W. Pree, BlenSor: Blender Sensor Simulation Toolbox, in *Advances in Visual Comput-*  
482 *ing, Lecture Notes in Computer Science*, vol. 6939, edited by G. Bebis, R. Boyle, B. Parvin, D. Koracin, S. Wang, K. Kyung-  
483 nam, B. Benes, K. Moreland, C. Borst, S. DiVerdi, C. Yi-Jen, and J. Ming, pp. 199–208, Springer Berlin Heidelberg, Berlin,  
484 Heidelberg, doi:[https://doi.org/10.1007/978-3-642-24031-7\\_20](https://doi.org/10.1007/978-3-642-24031-7_20), 2011.
- 485 Hackenberg, J., K. Calders, M. Demol, P. Raunonen, A. Piboule, and M. Disney, SimpleForest – a comprehensive tool for 3d  
486 reconstruction of trees from forest plot point clouds, doi:<https://doi.org/10.1101/2021.07.29.454344>, 2021.
- 487 Hämmerle, M., N. Lukač, K.-C. Chen, Z. Koma, C.-K. Wang, K. Anders, and B. Höfle, Simulating various terrestrial and  
488 UAV LIDAR scanning configurations for understory forest structure modelling, *ISPRS Annals of the Photogrammetry, Remote  
489 Sensing and Spatial Information Sciences*, IV-2/W4, 59–65, doi:<https://doi.org/10.5194/isprs-annals-IV-2-W4-59-2017>, 2017.
- 490 Henniger, H., A. Huth, K. Frank, and F. J. Bohn, Creating virtual forests around the globe and analysing their state space,  
491 *Ecological Modelling*, 483, 110,404, doi:<https://doi.org/10.1016/j.ecolmodel.2023.110404>, 2023.
- 492 Herrero-Huerta, M., R. Lindenbergh, and W. Gard, Leaf movements of indoor plants monitored by terrestrial LiDAR, *Frontiers  
493 in plant science*, 9, 189, doi:<https://doi.org/10.3389/fpls.2018.00189>, 2018.
- 494 Hopkinson, C., The influence of flying altitude, beam divergence, and pulse repetition frequency on laser pulse return intensity  
495 and canopy frequency distribution, *Canadian Journal of Remote Sensing*, 33(4), 312–324, doi:[https://doi.org/10.5589/m07-  
496 029](https://doi.org/10.5589/m07-029), 2007.
- 497 Huang, J., T. Birdal, Z. Gojcic, L. J. Guibas, and S.-M. Hu, Multiway Non-Rigid Point Cloud Registration via Learned  
498 Functional Map Synchronization, *IEEE transactions on pattern analysis and machine intelligence*, 45(2), 2038–2053,  
499 doi:<https://doi.org/10.1109/TPAMI.2022.3164653>, 2023.
- 500 Jackson, T. D., et al., The motion of trees in the wind: a data synthesis, *Biogeosciences*, 18(13), 4059–4072,  
501 doi:<https://doi.org/10.5194/bg-18-4059-2021>, 2021.

- 502 Jacobs, M., T. Hilmers, B. M. L. Leroy, H. Lemme, S. Kienlein, J. Müller, W. W. Weisser, and H. Pretzsch, Assessment of  
503 defoliation and subsequent growth losses caused by *Lymantria dispar* using terrestrial laser scanning (TLS), *Trees*, 36(2),  
504 819–834, doi:<https://doi.org/10.1007/s00468-021-02255-z>, 2022.
- 505 Jaeger, D. M., A. Looze, M. S. Raleigh, B. W. Miller, J. M. Friedman, and C. A. Wessman, From flowering to foliage: Ac-  
506 celerometers track tree sway to provide high-resolution insights into tree phenology, *Agricultural and Forest Meteorology*, 318,  
507 108,900, doi:<https://doi.org/10.1016/j.agrformet.2022.108900>, 2022.
- 508 Jiang, H., R. Hu, G. Yan, S. Cheng, F. Li, J. Qi, L. Li, D. Xie, and X. Mu, Influencing Factors in Estimation of  
509 Leaf Angle Distribution of an Individual Tree from Terrestrial Laser Scanning Data, *Remote Sensing*, 13(6), 1159,  
510 doi:<https://doi.org/10.3390/rs13061159>, 2021.
- 511 Junttila, S., M. Holopainen, M. Vastaranta, P. Lyytikäinen-Saarenmaa, H. Kaartinen, J. Hyypä, and H. Hyypä, The potential of  
512 dual-wavelength terrestrial lidar in early detection of *Ips typographus* (L.) infestation – Leaf water content as a proxy, *Remote*  
513 *Sensing of Environment*, 231, 111,264, doi:<https://doi.org/10.1016/j.rse.2019.111264>, 2019.
- 514 Kattenborn, T., R. Richter, C. GuimarãesSteinicke, H. Feilhauer, and C. Wirth, AngleCam : Predicting the temporal variation  
515 of leaf angle distributions from image series with deep learning, *Methods in Ecology and Evolution*, 13(11), 2531–2545,  
516 doi:<https://doi.org/10.1111/2041-210X.13968>, 2022.
- 517 Knapp, N., R. Fischer, and A. Huth, Linking lidar and forest modeling to assess biomass estimation across scales and disturbance  
518 states, *Remote Sensing of Environment*, 205, 199–209, doi:<https://doi.org/10.1016/j.rse.2017.11.018>, 2018.
- 519 Koenig, K., and B. Höfle, Full-Waveform Airborne Laser Scanning in Vegetation Studies – A Review of Point Cloud and Wave-  
520 form Features for Tree Species Classification, *Forests*, 7(9), 198, doi:<https://doi.org/10.3390/f7090198>, 2016.
- 521 Koetz, B., F. Baret, H. Poilvé, and J. Hill, Use of coupled canopy structure dynamic and radiative trans-  
522 fer models to estimate biophysical canopy characteristics, *Remote Sensing of Environment*, 95(1), 115–124,  
523 doi:<https://doi.org/10.1016/j.rse.2004.11.017>, 2005.
- 524 Lecigne, B., S. Delgrange, and O. Taugourdeau, Annual shoot segmentation and physiological age classification from TLS data  
525 in trees with acrotonic growth, *Forests*, 12(4), 391, doi:<https://doi.org/10.3390/f12040391>, 2021.
- 526 Lewis, P., Three-dimensional plant modelling for remote sensing simulation studies using the Botanical Plant Modelling System,  
527 *Agronomie*, 19(3-4), 185–210, doi:<https://doi.org/10.1051/agro:19990302>, 1999.
- 528 Li, B., J. Kałużny, J. Klein, D. L. Michels, W. Pałubicki, B. Benes, and S. Pirk, Learning to reconstruct botanical trees from  
529 single images, *ACM Transactions on Graphics*, 40(6), 1–15, doi:<https://doi.org/10.1145/3478513.3480525>, 2021a.
- 530 Li, C., O. Deussen, Y.-Z. Song, P. Willis, and P. Hall, Modeling and generating moving trees from video, in *Proceedings of*  
531 *the 2011 SIGGRAPH Asia Conference*, pp. 1–12, ACM, New York, NY, USA, doi:<https://doi.org/10.1145/2024156.2024161>,  
532 2011.
- 533 Li, L., X. Mu, M. Soma, P. Wan, J. Qi, R. Hu, W. Zhang, Y. Tong, and G. Yan, An iterative-mode scan design of terrestrial laser  
534 scanning in forests for minimizing occlusion effects, *IEEE Transactions on Geoscience and Remote Sensing*, 59(4), 3547–3566,  
535 doi:<https://doi.org/10.1109/TGRS.2020.3018643>, 2021b.

- 536 Li, W., X. Hu, Y. Su, S. Tao, Q. Ma, and Q. Guo, A new method for voxel-based modelling of three-dimensional for-  
537 est scenes with integration of terrestrial and airborne LiDAR data, *Methods in Ecology and Evolution*, 15(3), 569–582,  
538 doi:<https://doi.org/10.1111/2041-210X.14290>, 2024.
- 539 Li, Y., and T. Harada, Leopard: Learning partial point cloud matching in rigid and deformable scenes, in  
540 2022 *IEEE/CVF Conference on Computer Vision and Pattern Recognition (CVPR)*, pp. 5544–5554, IEEE,  
541 doi:<https://doi.org/10.1109/CVPR52688.2022.00547>, 2022.
- 542 Li, Y., X. Fan, N. J. Mitra, D. Chamovitz, D. Cohen-Or, and B. Chen, Analyzing growing plants from 4D point cloud data, *ACM*  
543 *Transactions on Graphics*, 32(6), 1–10, doi:<https://doi.org/10.1145/2508363.2508368>, 2013.
- 544 Liang, X., et al., Close-Range Remote Sensing of Forests: The state of the art, challenges, and oppor-  
545 tunities for systems and data acquisitions, *IEEE Geoscience and Remote Sensing Magazine*, 10(3), 32–71,  
546 doi:<https://doi.org/10.1109/MGRS.2022.3168135>, 2022.
- 547 Lintermann, B., and O. Deussen, Interactive modeling of plants, *IEEE Computer Graphics and Applications*, 19(1), 56–65,  
548 doi:<https://doi.org/10.1109/38.736469>, 1999.
- 549 Liu, J., A. K. Skidmore, T. Wang, X. Zhu, J. Premier, M. Heurich, B. Beudert, and S. Jones, Variation of leaf angle distribution  
550 quantified by terrestrial LiDAR in natural european beech forest, *ISPRS Journal of Photogrammetry and Remote Sensing*, 148,  
551 208–220, doi:<https://doi.org/10.1016/j.isprsjprs.2019.01.005>, 2019.
- 552 Liu, J., D. Wang, H. Gong, C. Wang, J. Zhu, and D. Wang, Advancing the understanding of fine-grained 3D forest structures  
553 using digital cousins and simulation-to-reality: Methods and datasets, doi:<https://doi.org/10.48550/arXiv.2501.03637>, 2025.
- 554 Liu, X., Q. Ma, X. Wu, T. Hu, Z. Liu, L. Liu, Q. Guo, and Y. Su, A novel entropy-based method to quantify for-  
555 est canopy structural complexity from multiplatform lidar point clouds, *Remote Sensing of Environment*, 282, 113,280,  
556 doi:<https://doi.org/10.1016/j.rse.2022.113280>, 2022.
- 557 Luo, Y., D. Xie, J. Qi, K. Zhou, G. Yan, and X. Mu, LESS LiDAR: A Full-Waveform and Discrete-Return Multispectral LiDAR  
558 Simulator Based on Ray Tracing Algorithm, *Remote Sensing*, 15(18), 4529, doi:<https://doi.org/10.3390/rs15184529>, 2023.
- 559 Makowski, M., T. Hädrich, J. Scheffczyk, D. L. Michels, S. Pirk, and W. Pałubicki, Synthetic silviculture, *ACM Transactions on*  
560 *Graphics*, 38(4), 1–14, doi:<https://doi.org/10.1145/3306346.3323039>, 2019.
- 561 Manivasagam, S., I. A. Bârsan, J. Wang, Z. Yang, and R. Urtasun, Towards Zero Domain Gap: A Comprehensive Study of  
562 Realistic LiDAR Simulation for Autonomy Testing, in 2023 *IEEE/CVF International Conference on Computer Vision (ICCV)*,  
563 pp. 8238–8248, IEEE, Paris, France, doi:<https://doi.org/10.1109/ICCV51070.2023.00760>, 2023.
- 564 Medic, T., J. Bömer, and S. Paulus, Challenges and recommendations for 3D plant phenotyping in agriculture using terrestrial  
565 lasers scanners, *ISPRS Annals of the Photogrammetry, Remote Sensing and Spatial Information Sciences*, X-1/W1-2023, 1007–  
566 1014, doi:<https://doi.org/10.5194/isprs-annals-X-1-W1-2023-1007-2023>, 2023.
- 567 North, P. R. J., Three-dimensional forest light interaction model using a Monte Carlo method, *IEEE Transactions on Geoscience*  
568 *and Remote Sensing*, 34(4), 946–956, doi:<https://doi.org/10.1109/36.508411>, 1996.
- 569 North, P. R. J., J. A. B. Rosette, J. C. Suárez, and S. O. Los, A Monte Carlo radiative transfer model of satellite waveform LiDAR,  
570 *International Journal of Remote Sensing*, 31(5), 1343–1358, doi:<https://doi.org/10.1080/01431160903380664>, 2010.

- 571 Ouaknine, A., T. Kattenborn, E. Laliberté, and D. Rolnick, OpenForest: a data catalog for machine learning in forest monitoring,  
572 *Environmental Data Science*, 4, e15, doi:<https://doi.org/10.1017/eds.2024.53>, 2025.
- 573 Palubicki, W., M. Makowski, W. Gajda, T. Hädrich, D. L. Michels, and S. Pirk, Ecoclimates: Climate-response modeling of  
574 vegetation, *ACM Transactions on Graphics*, 41(4), doi:<https://doi.org/10.1145/3528223.3530146>, 2022.
- 575 Pirk, S., T. Niese, O. Deussen, and B. Neubert, Capturing and animating the morphogenesis of polygonal tree models, *ACM*  
576 *Transactions on Graphics*, 31(6), 169:1–169:10, doi:<https://doi.org/10.1145/2366145.2366188>, 2012.
- 577 Pirk, S., T. Niese, T. Hädrich, B. Benes, and O. Deussen, Windy trees, *ACM Transactions on Graphics*, 33(6), 1–11,  
578 doi:<https://doi.org/10.1145/2661229.2661252>, 2014.
- 579 Porté, A., and H. H. Bartelink, Modelling mixed forest growth: a review of models for forest management, *Ecological Modelling*,  
580 150(1-2), 141–188, doi:[https://doi.org/10.1016/S0304-3800\(01\)00476-8](https://doi.org/10.1016/S0304-3800(01)00476-8), 2002.
- 581 Puliti, S., et al., Benchmarking tree species classification from proximally sensed laser scanning data: Introducing the FOR –  
582 species20K dataset, *Methods in Ecology and Evolution*, doi:<https://doi.org/10.1111/2041-210X.14503>, 2025.
- 583 Puttonen, E., et al., A Clustering Framework for Monitoring Circadian Rhythm in Structural Dynamics in Plants From Terrestrial  
584 Laser Scanning Time Series, *Frontiers in plant science*, 10, 486, doi:<https://doi.org/10.3389/fpls.2019.00486>, 2019.
- 585 Qi, J., D. Xie, T. Yin, G. Yan, J.-P. Gastellu-Etchegorry, L. Li, W. Zhang, X. Mu, and L. K. Norford, LESS: Large-Scale remote  
586 sensing data and image simulation framework over heterogeneous 3D scenes, *Remote Sensing of Environment*, 221, 695–706,  
587 doi:<https://doi.org/10.1016/j.rse.2018.11.036>, 2019.
- 588 Raunonen, P., M. Kaasalainen, M. Åkerblom, S. Kaasalainen, H. Kaartinen, M. Vastaranta, M. Holopainen, M. Disney, and  
589 P. Lewis, Fast Automatic Precision Tree Models from Terrestrial Laser Scanner Data, *Remote Sensing*, 5(2), 491–520,  
590 doi:<https://doi.org/10.3390/rs5020491>, 2013.
- 591 Raverta Capua, F., J. Schandin, and P. de Cristóforis, Training Point-Based Deep Learning Networks for Forest Segmentation  
592 with Synthetic Data, in *Pattern Recognition, Lecture Notes in Computer Science*, vol. 15304, edited by A. Antonacopoulos,  
593 S. Chaudhuri, R. Chellappa, C.-L. Liu, S. Bhattacharya, and U. Pal, pp. 64–80, Springer Nature Switzerland, Cham,  
594 doi:[https://doi.org/10.1007/978-3-031-78128-5\\_5](https://doi.org/10.1007/978-3-031-78128-5_5), 2025.
- 595 Reitmann, S., L. Neumann, and B. Jung, BLINDER-a blender AI add-on for generation of semantically labeled depth-sensing  
596 data, *Sensors (Basel, Switzerland)*, 21(6), doi:<https://doi.org/10.3390/s21062144>, 2021.
- 597 Roberts, O., P. Bunting, A. Hardy, and D. McInerney, Sensitivity analysis of the DART model for forest mensuration with airborne  
598 laser scanning, *Remote Sensing*, 12(2), 247, doi:<https://doi.org/10.3390/rs12020247>, 2020.
- 599 Rott, R., Dynamic Update of Stand-Alone LiDAR Model Based on Ray Tracing Using the Nvidia Op-  
600 tix Engine, in *2022 International Conference on Connected Vehicle and Expo (ICCVE)*, pp. 1–6, IEEE,  
601 doi:<https://doi.org/10.1109/ICCVE52871.2022.9743000>, 2022.
- 602 Schäfer, J., H. Weiser, L. Winiwarter, B. Höfle, S. Schmidlein, and F. E. Fassnacht, Generating synthetic laser scanning data of  
603 forests by combining forest inventory information, a tree point cloud database and an open-source laser scanning simulator,  
604 *Forestry: An International Journal of Forest Research*, 96(5), 653–671, doi:<https://doi.org/10.1093/forestry/cpad006>, 2023.

- 605 Schäfer, J., et al., Assessing the potential of synthetic and ex situ airborne laser scanning and ground plot  
606 data to train forest biomass models, *Forestry: An International Journal of Forest Research*, 97(4), 512–530,  
607 doi:<https://doi.org/10.1093/forestry/cpad061>, 2024.
- 608 Schmitt, S., G. Salzet, F. J. Fischer, I. Maréchaux, and J. Chave, rcontroll : An R interface for the individual-based forest dynam-  
609 ics simulator TROLL, *Methods in Ecology and Evolution*, 14(11), 2749–2757, doi:<https://doi.org/10.1111/2041-210X.14215>,  
610 2023.
- 611 Shcherbacheva, A., et al., A study of annual tree-wise LiDAR intensity patterns of boreal species observed using a hyper-temporal  
612 laser scanning time series, *Remote Sensing of Environment*, 305, 114,083, doi:<https://doi.org/10.1016/j.rse.2024.114083>, 2024.
- 613 Smelik, R. M., T. Tuteneel, R. Bidarra, and B. Benes, A survey on procedural modelling for virtual worlds, *Computer Graphics*  
614 *Forum*, 33(6), 31–50, doi:<https://doi.org/10.1111/cgf.12276>, 2014.
- 615 Smith, A. R., Plants, fractals, and formal languages, in *Proceedings of the 11th annual conference on Computer graphics and*  
616 *interactive techniques*, edited by D. A. Luther, R. M. Mueller, R. A. Weinberg, R. A. Ellis, and H. Christiansen, pp. 1–10,  
617 ACM, New York, NY, USA, doi:<https://doi.org/10.1145/800031.808571>, 1984.
- 618 Soudarissanane, S., R. Lindenbergh, M. Menenti, and P. Teunissen, Scanning geometry: Influencing factor on the  
619 quality of terrestrial laser scanning points, *ISPRS Journal of Photogrammetry and Remote Sensing*, 66(4), 389–399,  
620 doi:<https://doi.org/10.1016/j.isprsjprs.2011.01.005>, 2011.
- 621 Stava, O., S. Pirk, J. Kratt, B. Chen, R. Měch, O. Deussen, and B. Benes, Inverse procedural modelling of trees, *Computer*  
622 *Graphics Forum*, 33(6), 118–131, doi:<https://doi.org/10.1111/cgf.12282>, 2014.
- 623 Stocker, O., R. M. Kouhi, E. Guilbert, A. Ferraz, and T. Badard, Investigating the impact of point cloud density on semantic  
624 segmentation performance using virtual LiDAR in boreal forest, in *IGARSS 2023 - 2023 IEEE International Geoscience and*  
625 *Remote Sensing Symposium*, pp. 978–981, IEEE, doi:<https://doi.org/10.1109/IGARSS52108.2023.10282100>, 2023.
- 626 Stone, C., and C. Mohammed, Application of Remote Sensing Technologies for Assessing Planted Forests Damaged by Insect  
627 Pests and Fungal Pathogens: a Review, *Current Forestry Reports*, 3(2), 75–92, doi:<https://doi.org/10.1007/s40725-017-0056-1>,  
628 2017.
- 629 Sun, Z., R. Zhong, Q. Wu, and J. Guo, Airborne LiDAR Strip Adjustment Method Based on Point Clouds with Planar Neighbor-  
630 hoods, *Remote Sensing*, 15(23), 5447, doi:<https://doi.org/10.3390/rs15235447>, 2023.
- 631 Tan, P., T. Fang, J. Xiao, P. Zhao, and L. Quan, Single image tree modeling, *ACM Transactions on Graphics*, 27(5), 1–7,  
632 doi:<https://doi.org/10.1145/1409060.1409061>, 2008.
- 633 Tobin, J., R. Fong, A. Ray, J. Schneider, W. Zaremba, and P. Abbeel, Domain randomization for transferring deep neural networks  
634 from simulation to the real world, in *2017 IEEE/RSJ International Conference on Intelligent Robots and Systems (IROS)*, pp.  
635 23–30, IEEE, Vancouver, BC, doi:<https://doi.org/10.1109/IROS.2017.8202133>, 2017.
- 636 Tompalski, P., N. C. Coops, J. C. White, T. R. Goodbody, C. R. Hennigar, M. A. Wulder, J. Socha, and M. E. Woods, Estimating  
637 Changes in Forest Attributes and Enhancing Growth Projections: a Review of Existing Approaches and Future Directions  
638 using Airborne 3D Point Cloud Data, *Current Forestry Reports*, 7(1), 1–24, doi:<https://doi.org/10.1007/s40725-021-00135-w>,  
639 2021.

- 640 Vaaja, M. T., J.-P. Virtanen, M. Kurkela, V. Lehtola, J. Hyypä, and H. Hyypä, The effect of wind on tree stem parameter esti-  
641 mation using terrestrial laser scanning, *ISPRS Annals of Photogrammetry, Remote Sensing and Spatial Information Sciences*,  
642 *III-8*, 117–122, doi:<https://doi.org/10.5194/isprsannals-III-8-117-2016>, 2016.
- 643 Vicari, M. B., M. Disney, P. Wilkes, A. Burt, K. Calders, and W. Woodgate, Leaf and wood classification framework for terrestrial  
644 LiDAR point clouds, *Methods in Ecology and Evolution*, *10*(5), 680–694, doi:<https://doi.org/10.1111/2041-210X.13144>, 2019.
- 645 Wang, D., Unsupervised semantic and instance segmentation of forest point clouds, *ISPRS Journal of Photogrammetry and*  
646 *Remote Sensing*, *165*, 86–97, doi:<https://doi.org/10.1016/j.isprsjprs.2020.04.020>, 2020.
- 647 Wang, D., E. Puttonen, and E. Casella, PlantMove: A tool for quantifying motion fields of plant movements from  
648 point cloud time series, *International Journal of Applied Earth Observation and Geoinformation*, *110*, 102,781,  
649 doi:<https://doi.org/10.1016/j.jag.2022.102781>, 2022.
- 650 Weber, J., and J. Penn, Creation and rendering of realistic trees, in *Proceedings of the 22nd annual conference on Computer*  
651 *graphics and interactive techniques*, pp. 119–128, 1995.
- 652 Weiser, H., How does vegetation movement during laser scanning affect common point cloud-derived metrics? A virtual laser  
653 scanning study, M.Sc. thesis, Heidelberg University, Heidelberg, doi:<https://doi.org/10.11588/heidok.00035451>, 2024.
- 654 Weiser, H., L. Winiwarter, K. Anders, F. E. Fassnacht, and B. Höfle, Opaque voxel-based tree models for virtual laser scanning  
655 in forestry applications, *Remote Sensing of Environment*, *265*, 112,641, doi:<https://doi.org/10.1016/j.rse.2021.112641>, 2021.
- 656 Widlowski, J.-L., et al., The fourth phase of the radiative transfer model intercomparison (RAMI) exercise: Actual canopy  
657 scenarios and conformity testing, *Remote Sensing of Environment*, *169*, 418–437, doi:<https://doi.org/10.1016/j.rse.2015.08.016>,  
658 2015.
- 659 Wilkes, P., A. Lau, M. Disney, K. Calders, A. Burt, J. Gonzalez de Tanago, H. Bartholomeus, B. Brede, and M. Herold,  
660 Data acquisition considerations for Terrestrial Laser Scanning of forest plots, *Remote Sensing of Environment*, *196*, 140–153,  
661 doi:<https://doi.org/10.1016/j.rse.2017.04.030>, 2017.
- 662 Winiwarter, L., K. Anders, D. Schröder, and B. Höfle, Virtual laser scanning of dynamic scenes created from real 4D topographic  
663 point cloud data, *ISPRS Annals of the Photogrammetry, Remote Sensing and Spatial Information Sciences*, *V-2-2022*, 79–86,  
664 doi:<https://doi.org/10.5194/isprs-annals-V-2-2022-79-2022>, 2022a.
- 665 Winiwarter, L., A. M. Esmorís, H. Weiser, K. Anders, J. Martínez Sánchez, M. Searle, and B. Höfle, Virtual laser scanning with  
666 HELIOS++: A novel take on ray tracing-based simulation of topographic full-waveform 3D laser scanning, *Remote Sensing*  
667 *of Environment*, *269*, 112,772, doi:<https://doi.org/10.1016/j.rse.2021.112772>, 2022b.
- 668 Wittke, S., M. Campos, L. Ruoppa, R. Echriti, Y. Wang, A. Goloś, A. Kukko, J. Hyypä, and E. Puttonen, LiPheStream – A  
669 18-month high spatiotemporal resolution point cloud time series of Boreal trees from Finland, *Scientific data*, *11*(1), 1281,  
670 doi:<https://doi.org/10.1038/s41597-024-04143-w>, 2024.
- 671 Wu, B., G. Zheng, Y. Chen, and D. Yu, Assessing inclination angles of tree branches from terrestrial laser scan data us-  
672 ing a skeleton extraction method, *International Journal of Applied Earth Observation and Geoinformation*, *104*, 102,589,  
673 doi:<https://doi.org/10.1016/j.jag.2021.102589>, 2021.

- 674 Wulder, M. A., J. C. White, F. Alvarez, T. Han, J. Rogan, and B. Hawkes, Characterizing boreal for-  
675 est wildfire with multi-temporal Landsat and LIDAR data, *Remote Sensing of Environment*, 113(7), 1540–1555,  
676 doi:<https://doi.org/10.1016/j.rse.2009.03.004>, 2009.
- 677 Yu, Z., J. Qi, S. Liu, X. Zhao, and H. Huang, Evaluating forest aboveground biomass estimation model using simulated ALS  
678 point cloud from an individual-based forest model and 3D radiative transfer model across continents, *Journal of environmental*  
679 *management*, 372, 123,287, doi:<https://doi.org/10.1016/j.jenvman.2024.123287>, 2024.
- 680 Yun, T., M. P. Eichhorn, S. Jin, X. Yuan, W. Fang, X. Lu, X. Wang, and H. Zhang, A framework for phenotyping rubber trees  
681 under intense wind stress using laser scanning and digital twin technology, *Agricultural and Forest Meteorology*, 361, 110,319,  
682 doi:<https://doi.org/10.1016/j.agrformet.2024.110319>, 2025.
- 683 Zahs, V., K. Anders, J. Kohns, A. Stark, and B. Höfle, Classification of structural building damage grades from multi-temporal  
684 photogrammetric point clouds using a machine learning model trained on virtual laser scanning data, *International Journal of*  
685 *Applied Earth Observation and Geoinformation*, 122, 103,406, doi:<https://doi.org/10.1016/j.jag.2023.103406>, 2023.
- 686 Zanutto, F., S. Grigolato, D. Schindler, and L. Marchi, Identifying wind-tree dynamics with numerical simulations based on ex-  
687 perimental modal analysis, *Forest Ecology and Management*, 569, 122,188, doi:<https://doi.org/10.1016/j.foreco.2024.122188>,  
688 2024.
- 689 Zhao, K., J. C. Suarez, M. Garcia, T. Hu, C. Wang, and A. Londo, Utility of multitemporal lidar for forest and car-  
690 bon monitoring: Tree growth, biomass dynamics, and carbon flux, *Remote Sensing of Environment*, 204, 883–897,  
691 doi:<https://doi.org/10.1016/j.rse.2017.09.007>, 2018.
- 692 Zhao, X., J. Qi, H. Xu, Z. Yu, L. Yuan, Y. Chen, and H. Huang, Evaluating the potential of airborne hyperspectral LiDAR for  
693 assessing forest insects and diseases with 3D Radiative Transfer Modeling, *Remote Sensing of Environment*, 297, 113,759,  
694 doi:<https://doi.org/10.1016/j.rse.2023.113759>, 2023.
- 695 Zhao, Y., and J. Barbič, Interactive authoring of simulation-ready plants, *ACM Transactions on Graphics*, 32(4), 1–12,  
696 doi:<https://doi.org/10.1145/2461912.2461961>, 2013.
- 697 Zhou, X., B. Li, B. Benes, S. Fei, and S. Pirk, Deeptree: Modeling trees with situated latents, *IEEE Transactions on Visualization*  
698 *and Computer Graphics*, 30(8), 5795–5809, doi:<https://doi.org/10.1109/TVCG.2023.3307887>, 2024.
- 699 Zhu, X., J. Liu, A. K. Skidmore, J. Premier, and M. Heurich, A voxel matching method for effective leaf area index estimation  
700 in temperate deciduous forests from leaf-on and leaf-off airborne LiDAR data, *Remote Sensing of Environment*, 240, 111,696,  
701 doi:<https://doi.org/10.1016/j.rse.2020.111696>, 2020.
- 702 Zlinszky, A., B. Molnár, and A. S. Barfod, Not All Trees Sleep the Same – High Temporal Resolution Ter-  
703 restrial Laser Scanning Shows Differences in Nocturnal Plant Movement, *Frontiers in plant science*, 8, 1814,  
704 doi:<https://doi.org/10.3389/fpls.2017.01814>, 2017.